Biochimica et Biophysica Acta 1842 (2014) 1855–1869

Contents lists available at ScienceDirect

Biochimica et Biophysica Acta

journal homepage: www.elsevier.com/locate/bbadis

Changes in glutathione-dependent redox status and mitochondrial energetic strategies are part of the adaptive response during the filamentation process in *Candida albicans*

H. Guedouari [a], R. Gergondey [a], A. Bourdais [a], O. Vanparis [a], A.L. Bulteau [b], J.M. Camadro [a], F. Auchère [a,*]

[a] Laboratoire Mitochondries, Métaux et Stress Oxydant, Institut Jacques Monod, Université Paris-Diderot/CNRS (UMR 7592), 15 rue Hélène Brion, 75013 Paris, France
[b] IPREM-LCABIE UMR 5254, 2 rue du président Angot, 64000 Pau, France

ARTICLE INFO

Article history:
Received 6 February 2014
Received in revised form 4 July 2014
Accepted 6 July 2014
Available online 10 July 2014

Keywords:
Candida albicans
Glutathione
Oxidative stress
Mitochondria
Filamentation
Metabolism

ABSTRACT

Candida albicans is an opportunist pathogen responsible for a large spectrum of infections, from superficial mycosis to systemic diseases called candidiasis. Its ability to grow in various morphological forms, such as unicellular budding yeast, filamentous pseudohyphae and hyphae, contributes to its survival in the diverse microenvironments it encounters in the host. During infection *in vivo*, *C. albicans* is faced with high levels of reactive oxygen species (ROS) generated by phagocytes, and the thiol-dependent redox status of the cells reflects their levels of oxidative stress. We investigated the role of glutathione during the transition between the yeast and hyphal forms of the pathogen, in relation to possible changes in mitochondrial bioenergetic pathways. Using various growth media and selective mutations affecting the filamentation process, we showed that *C. albicans* filamentation was always associated with a depletion of intracellular glutathione levels. Moreover, the induction of hypha formation resulted in general changes in thiol metabolism, including the oxidation of cell surface −SH groups and glutathione excretion. Metabolic adaptation involved tricarboxylic acid (TCA) cycle activation, acceleration of mitochondrial respiration and a redistribution of electron transfer pathways, with an increase in the contribution of the alternative oxidase and rotenone-insensitive dehydrogenase. Changes in redox status and apparent oxidative stress may be necessary to the shift to adaptive metabolic pathways, ensuring normal mitochondrial function and adenosine triphosphate (ATP) levels. The consumption of intracellular glutathione levels during the filamentation process may thus be the price paid by *C. albicans* for survival in the conditions encountered in the host.

1. Introduction

Candida albicans is among the predominant fungal pathogens in humans and colonizes the mucosal surfaces of the oral and vaginal cavities and the digestive tract. It is a commensal on mucosal surfaces and in most cases does not cause any symptoms. However, it causes a broad range of infections, extending from superficial mycosis to life-threatening opportunistic bloodstream infections known as candidaemia, which can develop into disseminated candidiasis, principally in patients with compromised immunity [1–3]. A striking feature of *C. albicans* is its ability to grow in various morphological forms, including unicellular budding yeasts, filamentous pseudohyphae and true hyphae, and some less common forms, such as chlamydospores and opaque cells [1,4–7]. This ability to switch between forms is a key mechanism of survival in the hostile host environment [8–11]. Indeed, both hyphae and pseudohyphae are invasive and can promote tissue penetration in the early stages of infection, whereas the yeast form may be more suitable for dissemination in the bloodstream. Macrophages are more effective at engulfing yeast rather than hyphal forms and engulfment is influenced by hyphal length [12]. As a result, yeast cells can escape engulfment by macrophages by switching to the hyphal form [13].

Morphogenesis can be induced in various environmental conditions in *C. albicans in vitro* (for a review see [14,15]). Filamentation is enhanced at a temperature of 37 °C, in the presence of serum [16], in neutral or alkaline conditions [17], or in the presence of 5% CO_2 [18] or 1 mM N-acetyl-D-glucosamine [19]. In addition, hyphal growth is often induced in synthetic growth media, such as Lee's medium [20] or the semi-synthetic Spider medium [21]. The signaling pathways

Abbreviations: AOX, alternative oxidase; BSO, buthionine sulfoximide; CRC, classic respiratory chain; G6PDH, glucose-6-phosphate dehydrogenase; GLR, glutathione reductase; Gpx, glutathione peroxidase; Grx, glutaredoxin; GSH, reduced glutathione; GSSG, oxidized glutathione; GST, glutathione-S-transferase; IDP, isocitrate dehydrogenase; KGDH, α-ketoglutarate dehydrogenase; NAC, N-acetylcysteine; NADPH, β-nicotinamide adenine dinucleotide phosphate reduced form; PDH, pyruvate dehydrogenase; SHAM, salicylhydroxamic acid; YNB, yeast nitrogen base

* Corresponding author at: Laboratoire Mitochondries, Métaux et Stress Oxydant, Institut Jacques Monod, Université Paris-Diderot/CNRS, 15 rue Hélène Brion, 75013 Paris, France. Tel.: +33 1 57 27 80 28.
E-mail address: auchere.francoise@ijm.univ-paris-diderot.fr (F. Auchère).

http://dx.doi.org/10.1016/j.bbadis.2014.07.006
0925-4439/

transducing environmental signals into morphological switching are complex and have been studied extensively [14,22–24].

During infection *in vivo*, *C. albicans* cells are faced with high levels of ROS generated by phagocytes, and they have developed many adaptive antioxidant defenses, including glutathione-dependent systems (reviewed in [25]). *C albicans* is even more resistant to oxidative stress *in vitro* than the yeasts *Saccharomyces cerevisiae* and *Schizosaccharomyces pombe* [26,27]. Glutathione is an essential metabolite in almost all eukaryotic organisms and plays a key role in cellular resistance to oxidative damage [28,29]. The reduced sulfhydryl group in glutathione (GSH), when oxidized, produces a disulfide, or "oxidized glutathione" (GSSG) and, as a consequence, the GSH/GSSG ratio directly reflects intracellular redox changes. In *C. albicans*, the disruption of glutathione biosynthesis is associated with glutathione auxotrophy, higher ROS levels and lower levels of virulence [30,31]. Moreover, a significant decrease in glutathione levels has been observed after the thermal induction of hypha formation in Lee's medium (pH 6.5) or in the presence of serum [32–34]. Parallel changes in certain glutathione-dependent enzymes have been demonstrated [32,35,36], highlighting the importance of glutathione transferases in defense against phagocytes [37]. It has also recently been shown that cells lacking glutathione peroxidase Gpx3 cannot form filaments and are unable to escape from macrophages, and that the glutaredoxin Grx2 is required for virulence in a murine model [38,39]. These data suggest that the thiol redox status of the cells is involved in regulating the transition from yeast to hyphae.

C. albicans has evolved sophisticated mechanisms for sensing and adapting to oxidative conditions in the host. For instance, there are three mitochondrial respiratory pathways: the classic respiratory chain (CRC), the alternative terminal oxidase (AOX), the parallel respiratory chain (PAR), and two mitochondrial NADH dehydrogenases [40–43]. The CRC is the pathway providing the largest amount of cellular ATP and is the major source of respiratory activity and O_2 consumption. However, conflicting data have been published concerning the link between the respiratory machinery and filamentation, partly due to the diversity of experimental conditions used to stimulate dimorphism. Several early studies in *S. cerevisiae* and *C. albicans* showed that organisms with an intact respiratory pathway remained preferentially in the yeast form [44–46]. Respiratory blockade was subsequently shown to be associated with an increase in filamentation, as reported in [47]. However, surprisingly, the disruption of both alleles of the *C. albicans* NADH dehydrogenase Complex I (CaNdh51) gene has been reported to result in a filamentation defect [48]. The reintegration of a single copy of NDH51 restored filamentation, suggesting that this process may be associated with a functional respiratory chain. The same *ndh51* mutant has recently been shown to have 15 times the normal amount of pyruvate dehydrogenase complex (Pdx1), but with the same filamentation defect [49]. These data highlight the crucial importance of studies of metabolic pathways in the pathogen. However, the possible relationship between CRC, metabolic status and morphology in *C. albicans* remains poorly understood and the signal networks important for mitochondrial functions are also inadequately described.

In this study, we investigated the role of glutathione-dependent redox systems in dimorphic switching in *C. albicans*, in relation to major changes in mitochondrial bioenergetic pathways. We performed a complete biochemical analysis of the overall changes in cellular redox status and mitochondrial metabolism occurring during the filamentation process, by reliably inducing hyphae from unbudded yeast cells, by adding serum and incubating at 37 °C, and by growth in Spider medium in parallel. We obtained evidence for a severe disturbance of thiol metabolism in both filamentous forms, associated with a consumption of intracellular glutathione levels and apparent oxidative stress. Moreover, dynamic studies and experiments with mutants affected in the filamentation process (*ΔΔtup1* and *ΔΔefg1* mutants) confirmed that the adaptive response of *C. albicans* cells to hypha-inducing growth conditions involved glutathione. We also evaluated the cellular energetic cost of this response. The metabolic adaptation involved TCA cycle activation, complex I inhibition and a redistribution of the electron transfer pathways, with an increase in the contributions of the alternative oxidase and rotenone-insensitive dehydrogenase, to respond to the new energetic needs of the cells. Improvements in our understanding of the metabolic changes associated with the transition from the yeast to the hyphal form in *C. albicans* should provide insight into the complex strategies allowing this microorganism to adapt to the oxidative conditions encountered within the host.

2. Materials and methods

2.1. Yeast strains, media and growth conditions

The *C. albicans* wild-type virulent strain SC5314 [50] was routinely cultured at 30 °C in modified minimal YNB (yeast nitrogen base Difco, 2% D-glucose) supplemented with the necessary amino acids (pH 5.4). Hyphal growth was induced by culturing this strain in YNB medium supplemented with 10% fetal serum at 37 °C or in semi-synthetic Spider medium at 37 °C (Sigma) [3,21,51]. Cultures were carried out either in liquid medium with vigorous shaking on a rotary shaker or on medium solidified with 2% agar. We also used SLAD (synthetic low ammonium dextrose) medium where indicated. The other strains used in this study were BCa02-10 (*tup1Δ::hisG/tup1Δ::hisG::p405-URA3*, *ura3Δ::imm434/ura3Δ::imm434*) [52], Bca02-11 (*ΔΔTup1* rescue/TUP1-URA3) [52], SS4 (*efg1::ADE2/PCK1p::efg1 ura3Δ::imm434/ura3Δ::imm434*) [53] and CAI4 (*ura3Δ::imm434/ura3Δ::imm434/URA3-PCK1p::EFG1*) [54].

For dynamic experiments, yeast strains were cultured to early exponential growth phase and the cells were then collected by filtration and shifted to a new growth medium. Cells were collected from the culture medium at various times after resuspension in the new medium. For quorum sensing experiments, cells were cultured in YNB medium, YNB medium supplemented with 10% fetal bovine serum or Spider medium until reaching OD ~0.8 and collected by centrifugation.

2.2. Determination of protein content

We used the Bradford protein assay, with bovine serum albumin as the standard, to determine the protein content of cell extracts and isolated mitochondria. Enzyme activities are expressed per milligram of protein.

2.3. Preparation of C. albicans cell extracts

Yeast cells were cultured until an OD_{600nm} of 0.7 was reached, at which point they were harvested by centrifugation. Filamentous forms were subjected to sonication before OD measurement, to disrupt the filaments. The pellets were then resuspended in 50 mM potassium phosphate buffer pH 7.8 in the presence of protease inhibitors and the cells were disrupted with glass beads and centrifuged for 30 min at 5000 ×*g*. The supernatant was used as the crude cell extract.

2.4. Isolation of C. albicans mitochondria

C. albicans cells were cultured overnight in the appropriate medium and harvested by centrifugation at 4000 ×*g* for 10 min at 4 °C, washed with 50 ml of ice-cold water and resuspended in 0.6 M sorbitol and 50 mM Tris–HCl pH 7.5 supplemented with complete protease inhibitor mixture (Sigma). Cells were disrupted by vortexing with 0.45 mm-diameter sterile glass beads six times, for 30 s each, at two-minute intervals, on ice. All subsequent steps were carried out at 4 °C. Glass beads and unbroken cells were removed by centrifugation at 4000 ×*g* for 10 min, supernatants were centrifuged (14,000 ×*g*, 10 min, 4 °C) and the resulting pellets were resuspended in 0.6 M sorbitol and 50 mM Tris–HCl, pH 7.5, with the supernatants constituting the cytosolic fractions. Purified mitochondria were immediately frozen at −80 °C.

2.5. Determination of glutathione levels

Glutathione levels were determined with a modified version of the Tietze recycling enzymatic assay, as previously described [55]. For the estimation of total intracellular glutathione, samples were washed and resuspended in 50 mM potassium phosphate buffer pH 7.8 containing ice-cold 5% 5-sulfosalicylic acid. Specific glutathione content was calculated from standard curves obtained with various concentrations of GSSG, and is expressed in nmol of glutathione/mg of protein. This assay is based on the reduction of each GSSG molecule to give two GSH molecules, and the reading is in GSSG equivalents because GSSG is used as the standard, so the total measured specific glutathione content is 0.5 GSH + GSSG. For the quantification of oxidized glutathione (GSSG), samples (including GSSG standards) were treated with 2% (vol/vol) 4-vinylpyridine for 1 h at room temperature before analysis. The cytosolic and mitochondrial GSH/GSSG ratios were calculated as follows: GSH/GSSG = 2[(total glutathione) − GSSG] / GSSG.

2.6. Measurement of glutathione-dependent specific enzymatic activities

Glutathione peroxidase (Gpx) activity was assayed with a modified version of a previously described protocol, with tert-butyl hydroperoxide (t-BHP) as the substrate [56]. Glutathione reductase (GLR) activity was assayed by measuring the GSSG-dependent oxidation of NADPH, as reported in [26]. Glutathione-S-transferase (GST) activity was determined with GSH and with 1-chloro-2,4-dinitrobenzene (CDNB) as the secondary substrate, as previously described [57]. All results are reported relative to the protein concentration of the cell extract.

2.7. Quantification of reduced thiol —SH groups

Total reduced thiol content was determined by spectrophotometric quantification of the conversion of 5.5′-dithiobis-2-nitrobenzoic acid (DTNB) into 5-thio-2-nitrobenzoic acid (TNB) based on absorbance at 412 nm ($\varepsilon = 13.6\ mM^{-1}\ cm^{-1}$) in cell extracts (total intracellular free thiol groups) or entire cells (surface thiol groups) [58]. Free thiol groups were measured by the same protocol, in the supernatant after protein precipitation in TCA. Standard curves were obtained with various concentrations of GSH and/or cysteine concentrations and values are expressed in nmol of reduced thiol/mg of protein.

2.8. High performance liquid chromatography analysis of NADPH/$NADP^+$ pools

Following protein precipitation in TCA, we extracted $NADP^+$ in 0.5 M $HClO_4$ and NADPH in 0.5 M KOH, and reduced and oxidized nucleotides were then analyzed by reverse-phase HPLC [59]. Samples were injected onto a Zorbax C18 column (Agilent) at room temperature and the compounds were separated by a discontinuous gradient of 10 mM ammonium acetate buffer (pH 6.0)/methanol. The products were quantified by the integration of the peak absorbance area, using a calibration curve established with various known concentrations of NADPH and $NADP^+$.

2.9. Measurement of glucose-6-phosphate dehydrogenase activity

Glucose-6-phosphate dehydrogenase (G6PDH) activity was determined as previously described [60] and the results are expressed as nmol of NADPH/mg protein.

2.10. Assay for isocitrate dehydrogenase (IDP) activity

NADP-dependent IDP activity was measured in the cytosol and in freshly purified mitochondria. Mitochondria were diluted in 25 mM MOPS and 0.05% Triton X-100, pH 7.4, containing 2 mM $NADP^+$, 2 mM $MgCl_2$ and 5 mM isocitrate. Enzymatic activity was measured by evaluating NADPH production by monitoring absorbance at 340 nm ($\varepsilon = 6.2\ mM^{-1}\ cm^{-1}$). One unit of IDP was defined as the amount of enzyme catalyzing the production of 1 μmol of NADPH/min.

2.11. Assay for pyruvate dehydrogenase activity

Mitochondria were suspended in 25 mM MOPS and 0.05% Triton X-100, pH 7.4 supplemented with 1 mM $MgCl_2$, 5 mM NaF, and 1 mM $CaCl_2$, and pyruvate dehydrogenase activity was assayed spectrophotometrically as the rate of NAD (2.5 mM) reduction to NADH upon the addition of 4 mM pyruvate, 0.13 mM CoASH and 0.13 mM thiamine pyrophosphate, according to a modified version of a previously described procedure [61]. Before kinetic measurements, we added 8 μM rotenone to the reaction mixture to prevent the parallel oxidation of NADH by *C. albicans* NADH dehydrogenases. The results are expressed in nmol of reduced NADH/min/mg protein.

2.12. Assay for α-ketoglutarate dehydrogenase (KGDH) activity

Mitochondria were suspended in 25 mM MOPS and 0.05% Triton X-100, pH 7.4, and α-ketoglutarate dehydrogenase activity was assayed spectrophotometrically as the rate of NAD (1 mM) reduction to NADH upon the addition of 5 mM $MgCl_2$, 2.5 mM α-ketoglutarate, 0.1 mM CoASH and 0.2 mM thiamine pyrophosphate [55]. Before kinetic measurements, we added 8 μM rotenone to the reaction mixture to prevent parallel NADH oxidation by *C. albicans* NADH dehydrogenases. The results are expressed in nmol of reduced NADH/min/mg protein.

2.13. Assay for citrate synthase activity

The citrate synthase activity of freshly prepared mitochondria was assayed in a reaction mixture containing 100 mM Tris–HCl pH 8.0, 0.25 mM DTNB, 0.2 mM oxaloacetate and 0.1 mM acetyl-coA. The reaction was started by adding mitochondria and the reaction of free coenzyme A with DTNB to produce TNB was followed spectrophotometrically at 412 nm ($\varepsilon = 13.6\ mM^{-1}\ cm^{-1}$). The results are expressed in nmol of TNB/min/mg protein.

2.14. Assay for isocitrate lyase activity

Purified mitochondria were incubated in 100 mM potassium phosphate buffer pH 7.0, supplemented with 4 mM phenylhydrazine, 2.5 mM cysteine and 2.5 mM $MgCl_2$. The reaction was started by adding 2 mM isocitrate and the production of glyoxylate phenylhydrazone was followed at 324 nm ($\varepsilon = 19.3\ mM^{-1}\ cm^{-1}$). The results are expressed in nmol glyoxylate phenylhydrazone/min/mg protein.

2.15. Assay for mitochondrial electron respiratory chain (ERC) complexes

All assays were performed on isolated mitochondria. All spectrophotometric measurements were conducted on a Benchmark plus 96-well plate reader (Perkin Elmer). Complex I (NADH:ubiquinone oxidoreductase) activity was determined by adding 100 μl of assay buffer (35 mM NaH_2PO_4 pH 7.2, 5 mM $MgCl_2$, 0.25% BSA, 2 mM KCN, 1 μM antimycin, 97.5 μM ubiquinone-1, and 0.13 mM NADH) to 5 μg of mitochondrial protein. Activity was monitored by following NADH oxidation at 340 nm ($\varepsilon = 6.2\ mM^{-1}\ cm^{-1}$) and only the rotenone-sensitive activity was considered. Complex II (succinate dehydrogenase) activity was determined by adding 100 μl of assay buffer (25 mM KH_2PO_4, 5 mM $MgCl_2$, pH 7.2, 20 mM succinate, 50 μM DCPIP, 0.25% BSA, 2 mM KCN, and 1 μM antimycin) to 5 μg of mitochondrial protein. Enzymatic activity was monitored spectrophotometrically, by following the reduction of dichloroindophenol/phenazine ethosulfate (DCPIP/PES) at 600 nm ($\varepsilon = 19.1\ mM^{-1}\ cm^{-1}$). Complex IV (cytochrome *c* oxidase) activity was determined by following the oxidation of reduced cytochrome *c* at 550 nm ($\varepsilon = 18.5\ mM^{-1}\ cm^{-1}$), by adding 100 μl of assay buffer

(30 mM KH_2PO_4 pH 7.4, 1 mM EDTA, and 56 μM cytochrome *c*) to 5 μg of mitochondrial protein.

2.16. Mitochondrial respiration

The respiratory activity of isolated mitochondria was evaluated by an oxypolarographic method. The rate of oxygen consumption was measured in a 1 ml thermostatically controlled cell equipped with a Clark-type electrode, with Oxygraph plus V 1.01 software (Hansatech Instruments). The apparatus was calibrated with sodium dithionite before analysis. The oxygen consumption of isolated mitochondria was measured in 10 mM Tris–HCl buffer pH 6.8, supplemented with 0.65 M sorbitol, 0.36 mM EDTA, 10 mM KCl and 10 mM KH_2PO_4 and saturated with air at 30 °C (for the yeast form) or 37 °C (for the filamentous forms) (234 nmol O_2/ml). The electron donor for respiration was NADH (10 mM), succinate (10 mM), or pyruvate/malate (10 mM/2.5 mM). Rates of oxygen consumption are expressed in nmol oxygen/min/mg protein, and all values given are means of at least three determinations. For the quantification of oxygen consumption by different respiratory pathways, mitochondrial respiration was assayed in the presence of classical respiratory pathway inhibitors (10 μM rotenone, 10 mM KCN), whereas the AOX pathway was inhibited with 5 mM SHAM and 200 μM flavone was used to measure the contribution of the rotenone-insensitive NADH dehydrogenase to respiration.

2.17. Flow cytometry assays of ROS

Intracellular ROS production was detected by staining cells with the ROS-sensitive fluorescent dye DCFDA (2,7-dichlorofluorescein diacetate, Sigma) or DHE (dihydroethidium, Sigma) and assessing staining with a FACScan flow cytometer (488 nm) (Becton Dickinson). Cells were cultured overnight to a stationary phase, centrifuged for 3 min at 4000 ×*g*, washed and resuspended in PBS, and treated with 50 μM DCFDA for 30 min or 0.1 mg/ml DHE for 90 min in the dark. The cells were diluted, as appropriate, and fluorescence was measured immediately, only in living cells. Cell fluorescence in the absence of DCFDA or DHE was used to check that background fluorescence was similar in each strain, and the value obtained for untreated cells was subtracted from that obtained in each assay.

2.18. Mitochondrial ATP titration

ATP was quantified in freshly purified mitochondria with the Molecular Probes luminescence detection kit for ATP determination (Invitrogen). This assay is based on the requirement of ATP for light production by luciferase (emission maximum ~560 nm at pH 7.8) from the substrate luciferin. Freshly purified lysed mitochondria were added to the reaction mixture, which was shaken, and luminescence was then assessed immediately on a Spectramax microplate reader (Molecular Devices). ATP was quantified with a calibration curve established with various known concentrations of ATP. The results are expressed in pmol ATP/mg protein.

2.19. Statistical analysis

All data points in the figures, tables and data given are means of at least three independent determinations. Student's *t* test or non-parametrical Wilcoxon–Mann–Whitney test were used to identify significant differences.

3. Results

In this study, we used two experimental conditions to induce hypha formation in *C. albicans* SC5314 cells. These cells grow as a mixture of unicellular and budding yeast forms in minimal YNB medium at 30 °C (pH 5.4). The addition of serum and incubation at a temperature of 37 °C generates a signal for the induction of hypha formation [3,51]. We also used semi-synthetic Spider medium at 37 °C to induce the filamentation process, resulting in the production of both hyphae and pseudohyphae [21]. Pseudophyphae can be distinguished from true hyphae on the basis of their morphology, because pseudohyphae have constrictions at the septation sites and are wider than hyphae, whereas hyphae form long tube-like filaments with parallel sides (for a review see [15]). On solid medium, filamentation in YNB-serum results in a "cotton wool"-like appearance, whereas, in Spider medium, hypha formation leads to the development of feathery or spidery outgrowths from the main colony (Fig. 1A). The discrepancies reported in previous studies on *C. albicans* result partly from differences in the strains used and the diversity of experimental conditions used to stimulate dimorphism. In this text, we will refer to pseudohyphae and hyphae together as "filamentous forms".

3.1. Evidence for a consumption of intracellular glutathione during the yeast-to-hyphae transition

Glutathione levels were determined in *C. albicans* cell extracts, cytosols and purified mitochondria. Total glutathione levels in the cell extracts of both filamentous forms were much lower than those in the control cell extracts (Fig. 2A). Cytosolic and mitochondrial glutathione levels were also lower in filamentous cells, with a parallel decrease in

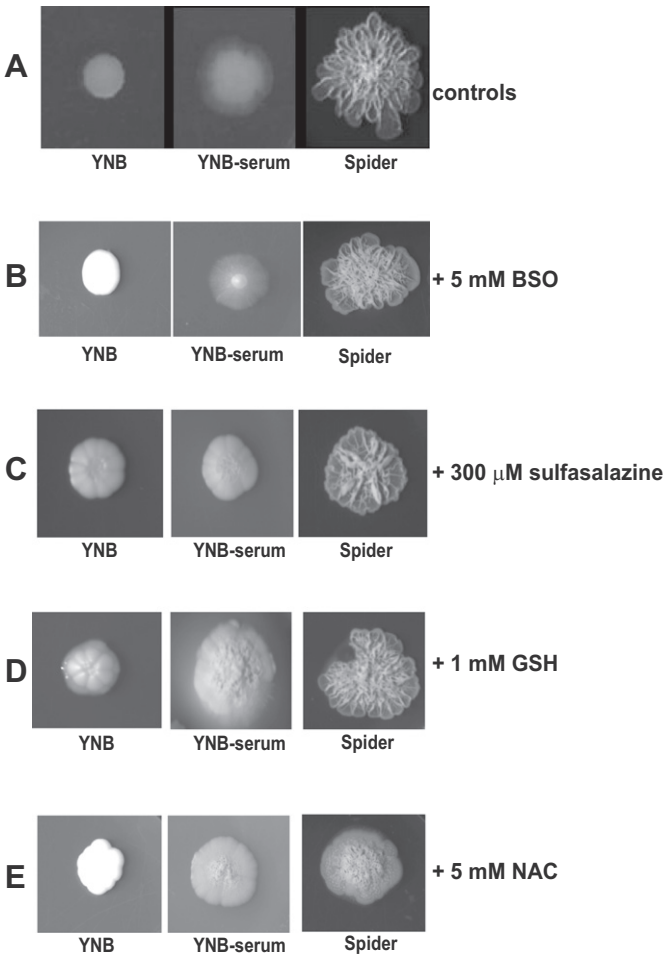

Fig. 1. Morphology of SC5314 *C. albicans* cells grown in various solid culture media. Cells were grown in A) YNB, YNB-serum and Spider media and the same media supplemented with B) 5 mM buthionine sulfoximide (BSO), C) 300 μM sulfasalazine, D) 1 mM reduced glutathione GSH and E) 5 mM N-acetylcysteine (NAC). Plates were inoculated at OD = 0.1 from an overnight culture and grown for 6 days at 30 °C (YNB medium) or 37 °C (YNB-serum and spider media).

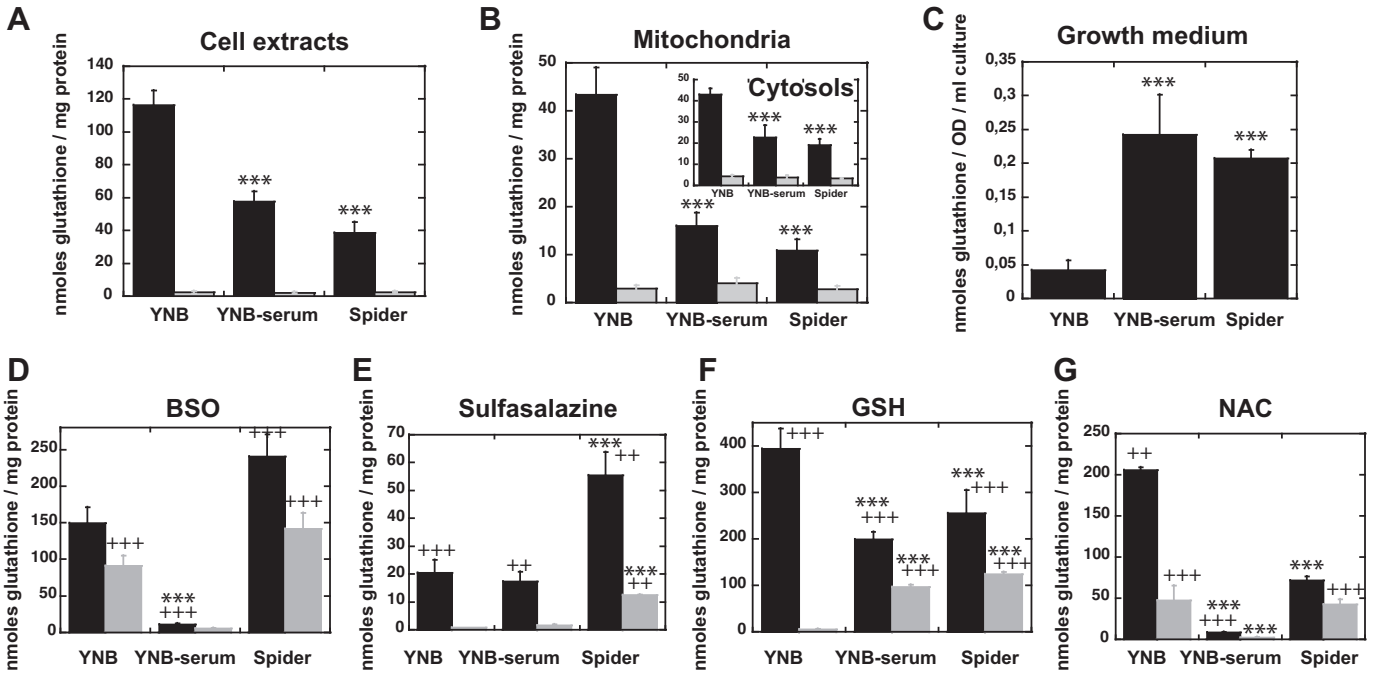

Fig. 2. Changes in intracellular glutathione levels in *C. albicans* cells grown in various culture media. Cells were cultured in YNB medium, YNB medium supplemented with 10% fetal bovine serum or Spider medium, and glutathione levels were determined as described in the Materials and methods section, in A) cell extracts and B) the cytosol and isolated mitochondria. Total glutathione levels are shown in black, and oxidized glutathione disulfide (GSSG) levels are shown in gray. C) Glutathione excretion into the culture medium. Panels D) to G) Total glutathione (black bars) and oxidized GSSG (gray bras) levels were determined in cellular extracts from cells grown in YNB, YNB-serum or Spider medium supplemented with D) 5 mM buthionine sulfoximide (BSO), E) 300 μM sulfasalazine, F) 1 mM GSH and G) 5 mM N-acetylcystein. All data points in the figure are the means ± SD of at least three determinations, normalized with respect to the protein content of the samples, and Student's *t* test was used to identify significant differences ($^{***}p < 0.001$ *versus* YNB), ($^{+++}p < 0.001$ *versus* untreated control), ($^{++}p < 0.01$ *versus* untreated control). In our experimental conditions, mitochondrial proteins accounted for 8% of cellular proteins and cytosolic proteins accounted for 92% of cellular proteins.

the GSH/GSSG ratios, falling from 20 in YNB medium, where glutathione is mainly in reduced form, to 6 in mitochondria in YNB-serum or Spider medium (Fig. 2B). Decreased GSH/GSSG ratios provide evidence for the occurrence of oxidative stress. A similar depletion of glutathione was observed when other conditions, such as low-ammonium SLAD medium were used to induce filamentation (Suppl. Data 1). The induction of filamentation also resulted in an increase in glutathione export (mainly in the reduced form) in the culture medium by a factor of four to five (Fig. 2C) and an increased binding of glutathione to proteins through glutathionylation (Suppl. Data 2).

To check whether glutathione depletion was a cause or a consequence of the filamentation process, similar experiments were performed in the presence of 5 mM buthionine sulfoximide (BSO), a known inhibitor of γ-glutamylcystenyl synthetase (γ-GCS), which catalyzes the first step of glutathione biosynthesis. Quite surprisingly, there was no significant change in glutathione levels in YNB medium, but a severe oxidative stress, reflected by the 1.3 value of the GSH/GSSG ratio, and no filamentation was observed in solid medium (Fig. 1B). The addition of higher BSO concentrations led to similar effects. In YNB-serum, we observed a severe depletion in glutathione, and a severe oxidative stress (GSH/GSSG ratio = 1.9), with parallel slight filamentation of the cells both in solid and liquid media (Fig. 1B and data not shown). We can hypothesize that cells are consuming all the glutathione produced to try to form hyphae. Inversely, in spider medium, there was an increase in glutathione levels, but a low GSH/GSSG ratio of 1.4, and cells were able to filament. Since spider is a rich growth medium, we cannot exclude that *C. albicans* cells were able to import glutathione from the external medium through glutathione transporters and/or mobilize intracellular cysteine stocks to produce glutathione in the presence of BSO.

In the presence of 300 μM sulfasalazine, which inhibits glutathione-S transferases (GST), there was a decrease in glutathione levels in both YNB and YNB-serum media compared to the controls (Fig. 2E), with no observation of hyphal formation (Fig. 1C). The perturbation of the glutathione metabolic pathway with sulfasalazine is thus associated with a glutathione-dependent intracellular oxidative stress, and an inhibition of hyphal formation in the presence of serum (Fig. 1C). These data suggest that a decrease in intracellular glutathione content does not constitute a signal for hyphal formation. A different behavior was observed in Spider medium, with glutathione levels similar to the ones observed in spider control cells, and a classic (or slightly perturbed) filamentation pattern (Fig. 1C). Since the inhibition of glutathione-S-transferase may partly inhibit glutathione export outside of the cell, these results suggest that, in spider medium, the filamentation process might involve glutathione export catalyzed by GST.

In parallel to experiments with BSO and sulfasalazine, which both affect glutathione metabolism, *C. albicans* cells were cultured in the presence of excess GSH or N-acetylcysteine (NAC). As expected, in the presence of 1 mM glutathione, we observed a large increase of intracellular glutathione content compared to the controls in our three experimental conditions (Fig. 2F). However, there was a glutathione depletion in both filamentous forms compared to the YNB, associated with a significant increase of oxidized GSSG, despite the excess of reduced glutathione added in the growth culture, with respective GSH/GSSG ratios of 2.1 and 2.4 in YNB-serum and spider media. In parallel, a classic filamentation pattern was observed in both hypha-inducing conditions, and a slight attempt of hyphal formation was even observed in YNB medium (Fig. 1 D). These results clearly show a consumption of reduced glutathione during the filamentation process. In the presence of 5 mM NAC, which can be a precursor for glutathione biosynthesis within the cells, glutathione content was increased in YNB medium, even though it did not reach the levels observed in the presence of GSH excess (Fig. 2G). In YNB-serum and spider conditions, glutathione levels were quite similar to the ones observed in the controls (Fig. 2A), but no or atypical filamentation was observed, even in Spider medium (Fig. 1E). Excess of NAC in the culture medium somehow stresses the cells and

might not be sufficient to compensate for the amount of glutathione consumed by the cells to form hyphae. Altogether, our results with BSO, sulfasalazine, GSH and NAC show that *C. albicans* cells need glutathione for filamentation but that glutathione depletion does not seem to elicit a signal for the filamentation process.

We explored the effect of filamentation on glutathione metabolism further, by measuring the activities of various glutathione-dependent enzymes (Table 1). We observed no significant change in glutathione peroxidase (Gpx) activity. Thus, the decrease in glutathione levels (Fig. 2) was not due to an increase in the consumption of reduced GSH to counteract an increase in intracellular ROS. However, we did observe increases in the specific activities of glutathione reductase (GLR; 3-fold increase) and glutathione transferase (GST; 5-fold increase) when filamentation was induced in Spider medium, probably in response to high GSSG levels. Our data also suggest that the export of glutathione observed in Spider medium may be catalyzed in part by GST, in response to changes in the GSH/GSSG ratio. This hypothesis was supported by our previous data of Fig. 2E and the fact that, in spider medium, excreted glutathione was decreased in the presence of sulfasalazine (data not shown).

3.2. Severe disturbance of general intracellular thiol redox status during the yeast-to-hyphae transition

The filamentation process was also found to be associated with a general disturbance of thiol metabolism (Table 2). Indeed, free reduced —SH groups (including glutathione and other non-protein thiols) levels were lower in both filamentous forms, with no change in the levels of protein —SH groups. Moreover, the induction of hypha formation was associated with a 2-fold decrease of the reduced exposed thiol groups, which are thought to be involved in cellular redox signaling, on the exofacial surface of the cells. We suggest that the depletion of the intracellular glutathione pool can change the redox balance of the cells through the oxidation of surface thiol groups, as previously reported for erythrocytes [62]. Changes to surface —SH groups (Table 2), glutathione excretion into the culture medium (Fig. 2) and GST activation in Spider medium (Table 1), may be involved in the adaptive response during morphogenesis.

3.3. Dynamic glutathione-dependent response of C. albicans cells to changes in growth conditions

We analyzed the possible involvement of glutathione in the adaptive response to environmental conditions further, by measuring total glutathione content when the cells were cultured in minimal YNB medium until reaching the exponential phase of growth and then transferred to new culture medium promoting filamentation. No change in the total glutathione pools was observed following shifting, after filtration, to the same YNB medium (Fig. 3A). This control is important to ensure that any changes in glutathione levels observed could be attributed to the experimental procedure itself.

Table 1
Specific activities of glutathione-dependent enzymes.
Cells were cultured in YNB medium, YNB medium supplemented with 10% fetal bovine serum or Spider medium, and specific enzymatic activities were measured as described in the Materials and methods. Each value in the table is the mean of at least three independent experiments, and Student's *t* test was used to identify significant differences.

	YNB	YNB-serum	Spider
Glutathione peroxidase (units/mg protein)	6321.0 ± 790.0	8709.5 ± 1340.8	8935.0 ± 1196.0
Glutathione reductase (units/mg protein)	1472.5 ± 114.6	1424.9 ± 354.0	3915.7 ± 885.8***
Glutathione transferase (units/mg protein)	10.1 ± 2.2	11.0 ± 1.9	52.3 ± 6.6***

*** $p < 0.001$ *versus* YNB.

After incubation for as little as 1 min in the new medium, glutathione content decreased by a factor of three, regardless of the conditions used to induce the filamentation process. After 1 h of growth in the new medium, the cells had begun to form filaments and no return to initial glutathione levels was observed (Fig. 3B and C). These findings show the existence of a rapid adaptation of *C. albicans* cells to new environmental hypha-inducing growth conditions, resulting in intracellular glutathione depletion, which is needed for hyphal formation.

3.4. Glutathione metabolism is affected in ΔΔefg1 and ΔΔtup1 mutants

We assessed the association of changes in glutathione levels with the yeast-to-hyphae transition, by measuring glutathione levels in two mutants affected in the filamentation process: *ΔΔtup1* and *ΔΔefg1* (Table 3). The general transcriptional corepressor Tup1 downregulates the expression of specific genes to inhibit hypha formation [52]. Cells lacking Tup1 repressor grow constitutively as long pseudohyphae. By contrast, the Efg1 protein upregulates certain genes in particular environmental conditions and cells lacking Efg1 present a filamentation defect [63]. Interestingly, it has been shown that the average time taken for the engulfment of an efg1 mutant by macrophages is longer than that of WT [12]. Table 3 shows that glutathione content of CAI4 WT cells was similar to the one observed in SC5314 WT cells in YNB and YNB-serum medium, but higher in spider medium, showing an effect of the genetic context in this growth medium. Glutathione levels of the *ΔΔefg1* mutant were unaffected in YNB compared to the WT, but displayed a 3-fold increase in YNB-serum, from 21.4 ± 1.9 to 61.6 ± 4.3 nmol glutathione/mg protein and, as expected, no filamentation was observed under those hypha-inducing conditions. Since cells do not need glutathione to form hyphae in the *ΔΔefg1* mutant, this might explain the higher glutathione levels. However, the mutation had no effect on glutathione content when cells were grown in Spider medium. Control experiments were performed on our *ΔΔefg1* strain using succinate as the main carbon source, taking advantage of the fact that the strain contains one deleted allele for efg1 and the other allele is under the control of a strong glucose-repressed promoter, making the strain functionally equivalent to a doubly deleted strain [53]. As described in [53], succinate 2% allows the expression of the repressed allele. The presence of succinate 2% led to the return to a slightly filamentous morphology of the mutant (in YNB-serum) and concomitant slight decrease in glutathione levels, although not reaching the levels observed in the presence of glucose 2% (Table 3).

When *ΔΔtup1* cells were cultured in YNB-serum medium, enhanced filamentation was accompanied by a large decrease in glutathione levels with respect to the yeast form (YNB) (Table 3). However, there was no significant effect on glutathione levels when cells were grown in Spider medium. Knowledge of the molecular mechanisms involved in the regulation of filamentation by Tup1 remains incomplete [14,15], but they are known to lead to pleiotropic effects on cells. However, the results displayed in Table 3 support the notion that genetic perturbation of filamentation pathways can be associated with disturbances of glutathione metabolism, and confirm that glutathione may be necessary for the yeast to hypha transition to occur.

3.5. Effect of quorum-sensing molecules on intracellular glutathione levels

It has recently been reported that the apoptosis induced by the quorum sensing molecule (QSM) farnesol in *C. albicans* is mediated by the depletion of intracellular glutathione [64]. *C. albicans* cells sense the density of the surrounding population by a quorum sensing mechanism mediated principally by farnesol, which is secreted into the environment and inhibits hyphal conversion and biofilm formation [65,66]. By contrast, the aromatic alcohol tyrosol shortens the lag phase of quiescent yeast cells and promotes germ-tube formation and hypha formation [67].

Table 2
Disturbance of general thiol metabolism in *C. albicans* filamentous forms.
Reduced thiol groups were quantified as described in the Materials and methods, by a reaction with DTNB to form TNB, absorbing at 412 nm, in *C. albicans* cell extracts and entire cells (cell surface exofacial thiol groups). Free reduced thiol groups were quantified in the supernatant after the precipitation of total protein in TCA. Each value in the table is the mean of at least five experiments, and Student's *t* test was used to identify significant differences.

	YNB	YNB-serum	Spider
Reduced total thiol groups (nmol/mg protein)	231.7 ± 30.2	95.1 ± 22.5***	114.9 ± 18.9***
Free reduced thiol groups (nmol/mg protein)	178.8 ± 35.5	58.0 ± 3.8***	70.2 ± 17.3***
Protein-SH groups (nmol/mg protein)	51.8 ± 11.2	39.8 ± 8.9	44.7 ± 4.5
Cell surface exofacial thiol groups (nmol/culture OD)	238.3 ± 51.7	140.4 ± 8.6***	113.9 ± 27.1***

*** $p < 0.001$ *versus* YNB.

We investigated the effect on glutathione metabolism of changes in the chemical environment, by adding 200 μM farnesol and 100 μM tyrosol to the same growth media used above and measuring intracellular glutathione levels (Fig. 4). Glutathione levels were unaffected by the addition of farnesol or tyrosol to YNB medium. However, in the presence of tyrosol, we observed a stimulation of hypha formation and a parallel decrease in glutathione levels in YNB-serum and Spider media. These results are consistent with the data shown in Fig. 2 and Table 3, indicating that enhanced filamentation is associated with a decrease in glutathione levels and that *C. albicans* cells need glutathione to produce hyphae. However, in the presence of the hyphal inhibitor farnesol, we also observed a significant decrease in total cellular glutathione content. These data are consistent with previous findings [64], but also confirm that a decrease in glutathione does not constitute a signal for filamentation, and that the intracellular depletion apparently associated with hyphal formation is a consequence of the filamentation process.

3.6. Inhibition of the pentose phosphate pathway and depletion of NADPH pools

Changes in thiol redox status may affect mitochondrial function and cellular energy metabolism. Most of the electrons required to maintain intracellular glutathione redox homeostasis are provided by NADPH. Indeed, glutathione reductases maintain the physiological GSH/GSSG balance by reducing GSSG in an NADPH-dependent reaction. We determined relative intracellular NADPH and $NADP^+$ levels in both yeast and filamentous cells, by reverse-phase HPLC. Reduced NADPH levels in filamentous forms were only one third to one half those of the yeast form (Fig. 5). In Spider medium, this depletion may be partly correlated to the increase in GLR activity reported in Table 1.

Glucose-6-phosphate dehydrogenase (G6PDH) was strongly inhibited in both filamentous forms, as shown by a comparison with the yeast form. G6PDH is the key enzyme of the pentose phosphate pathway responsible for NADPH production and is involved in protection against oxidative damage in eukaryotic cells. These results thus confirm that the filamentous forms of *C. albicans* are subject to oxidative stress. The inhibition of the pentose phosphate pathway also indicates a shift of cell metabolism toward glycolytic and energetic pathways. We observed a slight increase in NADP-dependent cytosolic isocitrate dehydrogenase activity (IDP2), but not sufficient to compensate for the depletion of the intracellular NADPH pool. In addition, the mitochondrial enzyme IDP1, catalyzing an alternative pathway of NADPH production, was strongly inhibited in filamentous forms.

3.7. Effect of filamentation on the activity of key mitochondrial enzymes of the TCA cycle

We explored the effect of filamentation on mitochondrial function further, by measuring the specific activities of key mitochondrial enzymes (Fig. 6). Pyruvate dehydrogenase, which acts upstream from the TCA cycle, was slightly activated in hypha-inducing conditions. The first TCA cycle enzyme, citrate synthase, was strongly induced in both sets of conditions used to promote hypha formation. Citrate synthase catalyzes the reactions driving the TCA cycle within the mitochondria. These results therefore suggest that the TCA cycle is stimulated during hypha formation. Citrate synthase activation is also necessary to respond to the energetic needs of the cell and to counterbalance the increase in glycolytic activity. We also observed a significant increase in KGDH activity during filamentation (Fig. 6), probably compensating for the severe inhibition of mitochondrial IDP (Fig. 5). As stated above, *C. albicans* has a high adaptation capacity, due to its three different respiratory chains and the existence of adaptive metabolic pathways. The glyoxylate cycle, which has several steps in common with the TCA cycle, makes it possible for this microorganism to use two-carbon compounds as carbon sources and has been implicated in virulence [68]. Isocitrate lyase was found to be inhibited in both filamentous forms (Fig. 6), consistent with the stimulation of KHDH activity. The concomitant activation of the classical TCA cycle and inhibition of the pentose phosphate pathway reflects a shift of the cells toward higher levels of energy production during the filamentation process, possibly as a way of providing the mitochondrial respiratory chain with a larger number of electrons.

3.8. Filamentation and mitochondrial respiration

Various studies have suggested that the filamentation process is intrinsically correlated with the presence of an intact and functional mitochondrial respiratory chain [48,49], but conflicting data have been published. We explored this aspect, by measuring oxygen consumption in isolated mitochondria, at 30 °C for the yeast forms and 37 °C for the filamentous forms, in the presence of three electron donors: NADH, succinate and pyruvate/malate (Table 4). When the pyruvate/malate mixture was used as a substrate, we observed a large increase in oxygen consumption in both filamentation-inducing conditions. Pyruvate/malate was the only substrate of the three tested that was entirely dependent on the integrity of TCA cycle enzyme functions for the provision of electrons to the mitochondrial respiratory chain. These results are therefore consistent with TCA cycle activation (Fig. 6) and reflect major metabolic changes associated with the filamentation process. These results were confirmed by additional polarography experiments on entire cells, with endogenous substrates or exogenous glucose (data not shown) as the respiratory substrate.

However, in the presence of NADH as an electron donor, we observed a decrease in mitochondrial oxygen consumption in both filamentous forms. In the presence of succinate, a different pattern was observed, with respiration decreasing only in YNB-serum medium. These data suggest that the general increase in oxygen consumption in the filamentous forms observed in the presence of pyruvate/malate may be associated with a change in the respective contributions of the *C. albicans* electron transfer chains, with a probable decrease in the contributions of the complex I and NADH dehydrogenases.

3.9. The alternative oxidase pathway is stimulated in the filamentous forms

Like various plants and fungi, *C. albicans* has an alternative terminal oxidase (AOX) that can accept electrons directly from coenzyme Q. However, some groups have called into question the utility of the AOX

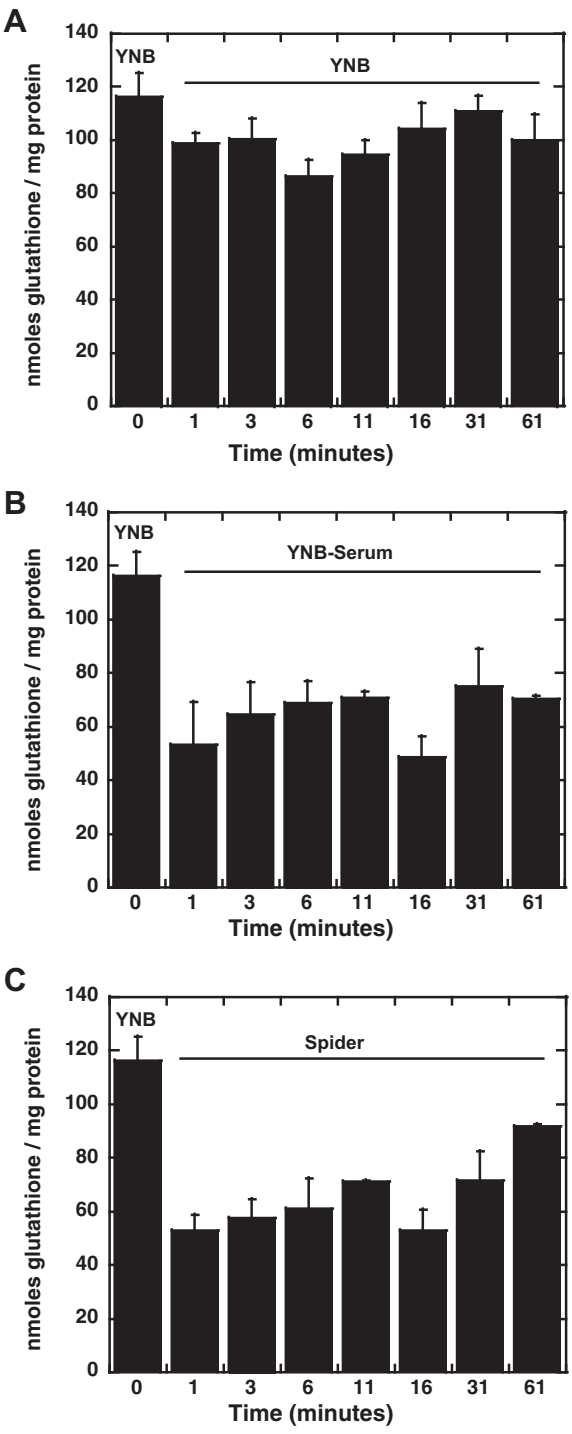

Fig. 3. Rapid dynamic glutathione-dependent adaptive response to changes in cell growth conditions. Cells were cultured to the exponential growth phase in YNB medium, isolated by filtration and shifted to different media: A) identical YNB medium; B) YNB medium supplemented with 10% serum; C) Spider medium. Samples were taken 0, 1, 3, 6, 11, 16, 31 and 61 min after cell filtration and transferred to the new growth medium, and total glutathione (GSH + GSSG) levels were determined by the recycling enzymatic assay. All data points in the figure are means ± SD of at least three determinations.

pathway, which cannot synthesize as much ATP as the classic chain, during filamentation in this pathogen. The contribution of the AOX pathway to total respiration was estimated by measuring both SHAM (salicylhydroxamic acid)-resistant (AOX) and potassium cyanide (KCN)-resistant respiration (parallel respiratory chain and complex IV from the classical respiratory chain (CRC)).

Table 3
Total glutathione levels in cell extracts of *C. albicans* WT SS4 cells and mutants with impaired filamentation signaling pathways.
Cells were cultured in YNB medium, YNB medium supplemented with 10% fetal bovine serum or Spider medium, and glutathione levels were determined in cell extracts as described in the Materials and methods. In the case of *ΔΔefg1* mutant, cells were cultured in the presence of 2% glucose or 2% succinate as main carbon sources. Each value in the table is the mean of at least five experiments, and Student's *t* test was used to identify significant differences.

	YNB	YNB-serum	Spider
	Nmol total glutathione/mg protein		
WT (CAI-4) (glucose 2%)	168.0 ± 6.5	21.4 ± 1.9***	130.0 ± 5.6
WT (CAI-4) (succinate 2%)	136.6 ± 5.2	22.4 ± 2.9***	–
ΔΔefg1 (glucose 2%)	148.8 ± 16.3	61.6 ± 4.3**,++	140.8 ± 4.2
ΔΔefg1 (succinate 2%)	167.5 ± 17.5	46.5 ± 2.0**,++	–
ΔΔTup1 (Bca02-10)	124.6 ± 15.9	22.6 ± 4.4***	166.6 ± 16.2
ΔΔTup1 rescue/TUP1-URA3 (Bca02-11)	114.7 ± 11.7	22.3 ± 3.9***	67.4 ± 14.6**

*** $p < 0.001$ *versus* YNB.
** $p < 0.01$ *versus* YNB.
++ $p < 0.01$ *versus* WT grown in similar conditions.

As illustrated in the polarographic profile presented in Fig. 7, oxygen consumption by isolated mitochondria results from the concomitant contributions of the various electron transfer pathways. Indeed, the addition of SHAM first, before the addition of cyanide, resulted in a partial decrease in respiratory rate, with only the subsequent addition of KCN resulting in a complete inhibition of respiration. The contribution of SHAM-resistant respiration was greater in the filamentous forms (Table 4). The AOX pathway accounted for about 25% of the total respiration in the yeast form, but more than 50% of electron transfer in both hypha-inducing conditions. Furthermore, the respiration on pyruvate/malate and external NADH was less rotenone-sensitive, and more sensitive to the addition of 200 μM flavone in YNB-serum and Spider media, suggesting a greater contribution of the alternative rotenone-insensitive NADH dehydrogenase. Electron transfer through AOX, NADH dehydrogenases and the parallel respiratory chain produces less ATP than the classical pathway. This phenomenon therefore reflects the potential of the cell to respond immediately to changes in energy demands in changing environmental conditions.

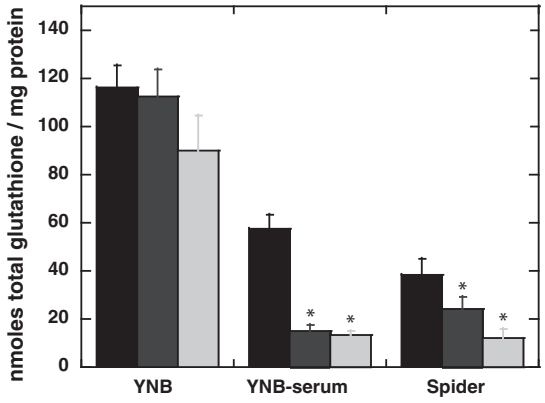

Fig. 4. Effect of quorum sensing molecules on intracellular glutathione levels in *C. albicans* grown in various media. Cells were cultured in YNB medium (30 °C), YNB medium supplemented with 10% fetal bovine serum (37 °C) or Spider medium (37 °C) until reaching OD ~ 0.8. Control cultures are shown in black, cultures supplemented with 200 μM farnesol are shown in dark gray and cultures supplemented with 100 μM tyrosol are shown in light gray. Total glutathione levels were determined in cell extracts, as described in the Materials and methods section, and all data points in the figure are means ± SD of at least three determinations and Wilcoxon–Mann–Whitney test was used to identify significant differences (* $p < 0.05$ *versus* YNB).

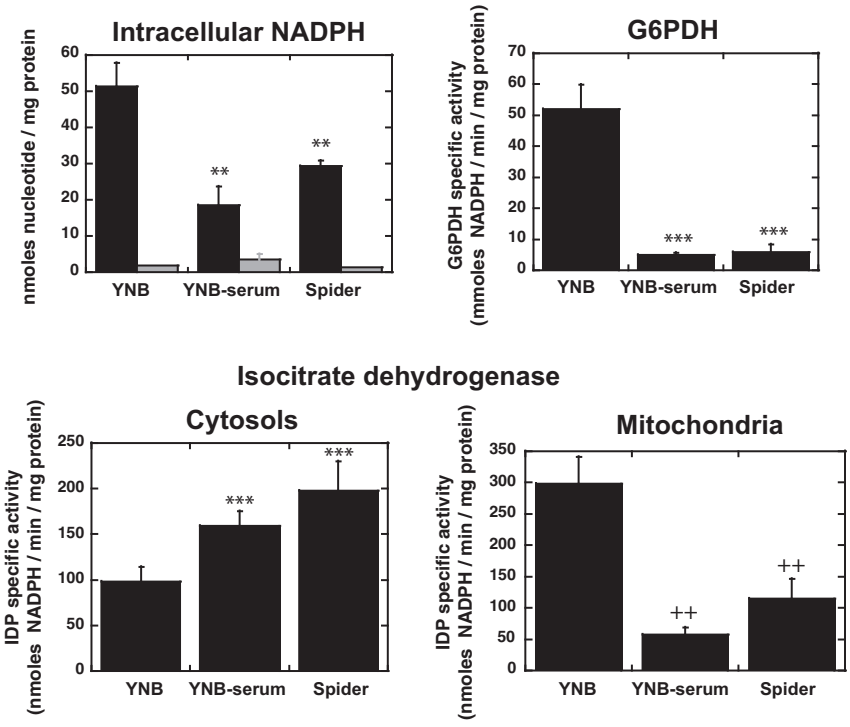

Fig. 5. Inhibition of the pentose phosphate pathway and depletion in intracellular NADPH in *C. albicans* filamentous forms. Glucose-6-phosphate dehydrogenase (G6PDH) and NADP-dependent isocitrate dehydrogenase (IDP) activities were assayed as described in the Materials and methods. After acidic or alkaline extraction, NADPH and $NADP^+$ levels were determined by reverse-phase HPLC. Products were monitored spectrophotometrically at 260 nm and quantified by integration of the peak absorbance area, based on a calibration curve of known concentrations of NADPH and $NADP^+$. All data points in the figure are the means ± SD of at least three determinations and normalized with respect to the protein content of the samples. Student's *t* test and Wilcoxon–Mann–Whitney test were used to identify significant differences ($^{*}p < 0.001$ and $^{**}p < 0.01$ *versus* YNB, $^{++}p < 0.05$).

3.10. Complex I inhibition and higher levels of ROS production in filamentous forms

On the basis of the results obtained in inhibitor studies, we determined the specific activities of individual enzymes from the ERC complexes (Table 5). Levels of rotenone-sensitive complex I specific activity, measured upon the addition of rotenone to the reaction mixture, in both sets of conditions inducing hypha production were only a quarter of those for the yeast form. We cannot rule out the possibility that a small proportion of the rotenone-sensitive activity detected in our assay can be accounted for by the internal rotenone-sensitive NADH dehydrogenase (NDE1). However, these results are consistent with the ERC inhibitor data shown in Table 4, suggesting a redistribution of the electron transfer pathways, with a minor contribution of rotenone-sensitive oxygen consumption. Moreover, the rotenone-insensitive activity detected in our complex I assay was of ~20 in yeast forms, and ~35 in filamentous forms, consistent with the apparent increase in the contribution of rotenone-insensitive dehydrogenase (YMX6). The succinate dehydrogenase activity of complex II remained unchanged, although a decrease of respiration was observed in YNB-serum in the presence of succinate (Table 4). We also observed an increase in complex IV activity, showing that the respiratory chain remains functional in these conditions, although levels of complex IV proteins remained unchanged during the filamentation process (western blot analysis, data not shown).

CRC dysfunction, concerning complex I in particular in fungi, is classically associated with an increase in ROS intracellular levels [69]. In addition, previous studies have shown that exponential hyphae are more resistant to oxidative stress than yeast cells while stationary phase filaments are more sensitive that stationary phase yeast cells [13,36]. Total cell ROS levels were determined by quantitative flow cytometry. The fluorescent dye 2′,7′-dichlorofluorescein diacetate (DCFDA) is widely used for the measurement of ROS levels in both mammalian and fungal cells, and dihydroethidium (DHE) is used specifically in superoxide anion assays. Intracellular ROS levels were higher when cells were cultured in YNB-serum and, to a lesser extent, in Spider medium, than in minimal YNB medium (Fig. 8), probably due to complex I defects and higher levels of oxidative stress. However, there was no significant change in 20S-proteasome activity, but an increase in protein-glutathione adducts, measured using a specific monoclonal anti-glutathione antibody, suggesting that a protein glutathionylation process may also be involved in the metabolic adaptation of *C. albicans* (Supplementary data 2 and unpublished data). (See Fig. 9.)

These changes in mitochondrial energetic metabolism associated with filamentation may modify ATP synthesis. However, intramitochondrial ATP levels remained constant (Fig. 8). A redistribution of electron transfer pathways would allow the microorganism to fine-tune ATP production without having to slow respiration, and to maintain ATP production at levels compatible with the promotion of hyphal growth and adaptation to oxidative environments within the host.

4. Discussion

In *C. albicans*, the filamentation process is part of the adaptive response to the new oxidative environment encountered within the host. An understanding of the molecular basis of this ability to adapt to different conditions requires studies of the metabolic pathways involved in *C. albicans* morphogenesis. In this study, we investigated the mitochondrial metabolic strategies employed during the yeast-to-hyphae transition, by exploring the concomitant biochemical changes in intracellular glutathione-dependent redox status and mitochondrial function after the induction of the filamentation process *in vitro* (Fig. 1).

Within the host, pathogens experience diverse stress conditions, including exposure to ROS and hypoxia, in which glutathione plays a particularly crucial role [70]. In *C. albicans*, various studies have suggested a possible role for glutathione in morphogenesis and virulence [32–39]. We found that glutathione levels decreased following the induction of

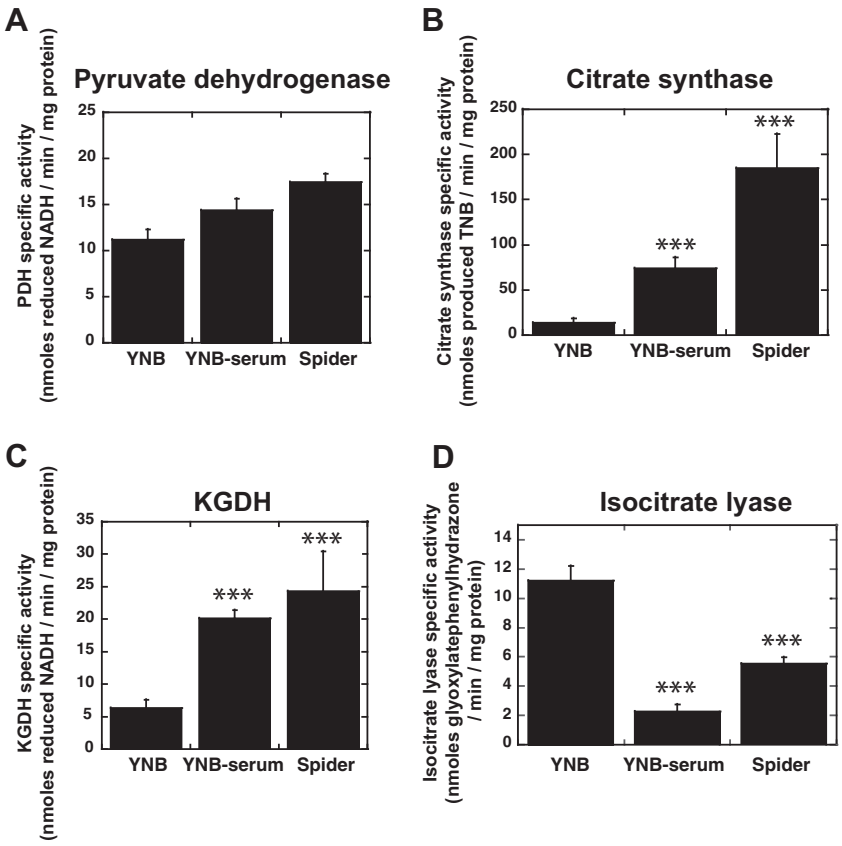

Fig. 6. Specific activities of key mitochondrial enzymes in *C. albicans* grown in different culture media. Cells were cultured in YNB medium, YNB medium supplemented with 10% fetal bovine serum or Spider medium. Mitochondria were then isolated and disrupted, and enzyme activities were determined as described in the Materials and methods. A) Pyruvate dehydrogenase activity, B) citrate synthase activity, C) α-ketoglutarate dehydrogenase activity, D) isocitrate lyase activity. All data points in the figure are the means of at least three determinations, normalized with respect to the protein content of the samples, and Student's *t* test was used to identify significant differences ($^{*}p < 0.01$ and $^{**}p < 0.01$ *versus* YNB).

the filamentation process (Fig. 2), with parallel cytosolic and mitochondrial oxidative stress (low GSH/GSSG ratios) and decrease in the number of reduced free thiol groups (Table 2). These findings are consistent with previous reports that GSH content decreases in actively growing cells during the initial steps of germ-tube formation during the yeast-to-hyphae transition, regardless of the nature of the stimulus inducing this transition (temperature or pH) [32–36].

In the presence of BSO, which inhibits the first enzyme of the glutathione biosynthesis pathway (γ-GCS), a severe decrease in glutathione levels and concomitant oxidative stress was observed in YNB-serum, with a slight attempt to hyphal formation. This strongly suggests that synthetized glutathione is consumed to try to produce hyphae. In Spider medium supplemented with BSO, intracellular glutathione levels were maintained to levels similar to the controls, and a classic filamentation pattern was observed but with the counterpart of oxidative stress (GSH/GSSG ratio = 1.4). Previous studies have shown that the presence of exogenous GSH is an absolute requirement for the γ-GCS mutant to grow [30,31]. *C. albicans* cells may import glutathione from the rich spider medium or synthesize glutathione from intracellular γ-glutamylcysteine stocks. We also cannot exclude that we observe a temporary burst of glutathione as an adaptive response to the BSO inhibitory effect, which might be followed by further glutathione depletion as a consequence of hyphal formation. However, since some of our data (Suppl. data 2 and unpublished results) suggest an increase in protein glutathionylation in Spider medium, a plausible explanation would be that higher glutathione levels may be the consequence of the reverse protein deglutathionylation which can generate pools of free glutathione in deprivation conditions such as the presence of BSO. We are currently running proteomic experiments to further explore the glutathionylation process in *C. albicans* filamentous cells. Our results also emphasize the differences in our two hypha-inducing growth conditions which would have to be explored further.

The depletion of intracellular GSH would be expected to activate glutathione-dependent enzymatic reactions, as a compensatory mechanism. Under our conditions, GST activity increased by a factor of five in Spider medium, suggesting a possible participation of this enzyme to the glutathione export observed in Fig. 2. Indeed, GST conjugates xenobiotics or their metabolites to glutathione, leading to the elimination of the conjugates or their internalization in cellular compartments, and an increase in transcription of the GST gene has been observed during germ-tube emergence [36]. In addition, some GST upregulation is observed in macrophages and neutrophils and may play an important role in counteracting the oxidative burst occurring within phagocytes [37]. The addition of sulfasalazine, which under our conditions, fully inhibits GST activity, led to a decrease in glutathione content both in YNB and YNB-serum media, but no filamentation was observed. This supports the hypothesis that intracellular glutathione depletion does not elicit the filamentation process. Inversely, in spider medium, GST blockage led to a slight increase in glutathione levels, in agreement with the increase in GST activity (Table 1) and a possible role of glutathione excretion catalyzed by GST in hyphal formation. This was supported by the lower amount of glutathione exported in the culture medium in the presence of sulfasalazine (data not shown). Glutathione-dependent enzymes such as GST might make attractive targets for antifungal therapy.

The addition of excess GSH in the cultures confirmed that hyphal formation was associated with a high consumption of reduced glutathione, and that the glutathione-dependent oxidative stress observed in the

Table 4
C. albicans mitochondrial respiration in the presence of various electron donors and in the presence of ETC inhibitors.
The oxygen consumption of isolated mitochondria (state 2 respiration) was measured as described in the Materials and methods, at 30 °C for the yeast forms and 37 °C for the filamentous forms, in the presence of various electron donors: NADH (10 mM), succinate (10 mM), or pyruvate/malate (10 mM/2.5 mM), and ETC inhibitors. We used 10 mM KCN to inhibit complex IV, 10 μM rotenone to inhibit complex I and rotenone-sensitive dehydrogenase, 200 μM flavone to inhibit the rotenone-insensitive NADH dehydrogenase and 5 mM SHAM to inhibit the alternative oxidase AOX. The rates of oxygen consumption are expressed in nmol oxygen/min/mg protein, and the values listed are means of at least three determinations.

Mitochondrial respiration (nmol O_2/min/mg protein)			
	NADH	Succinate	Pyruvate/malate
YNB			
No inhibitor	90.1 ± 16.1	50.8 ± 11.4	50.8 ± 11.4
% inhibition			
+5 mM SHAM	23.7 ± 7.6%	26.2 ± 3.2%	23.4 ± 5.8%
+10 μM rotenone	80.4 ± 16.8%	52.1 ± 2.3%	86%
+10 mM KCN	76.8 ± 6.3%	71.1 ± 1.1%	78.0 ± 1.1%
+200 μM flavone	11.0 ± 2.3%	8.4 ± 1.3%	8.8 ± 2.2%
YNB-serum			
No inhibitor	23.4 ± 1.6***	15.9 ± 2.5***	28.8 ± 14.7**
% inhibition			
+5 mM SHAM	46.9 ± 4.8%	54.3 ± 3.6%	62.9 ± 17.8%
+10 μM rotenone	51.2 ± 8.1%	48.1 ± 4.2%	35 ± 1.3%
+10 mM KCN	58.3 ± 4.2	52%	55%
+200 μM flavone	16.8 ± 4.3%	26.8 ± 2.3%	26.8 ± 6.3%
Spider			
No inhibitor	66.4 ± 8.5**	61.8 ± 13.7	54.0 ± 13.1***
% inhibition			
+5 mM SHAM	47 ± 6.8%	72.0 ± 16.8%	56.0 ± 8.6%
+10 μM rotenone	63.8 ± 2.2%	41.8 ± 2.9%	42 ± 2.8%
+10 mM KCN	44.0 ± 1.1%	38%	50%
+200 μM flavone	24.8 ± 3.3%	19.8 ± 5.3%	19.7 ± 4.2%

*** $p < 0.001$ *versus* YNB.
** $p < 0.01$ *versus* YNB.

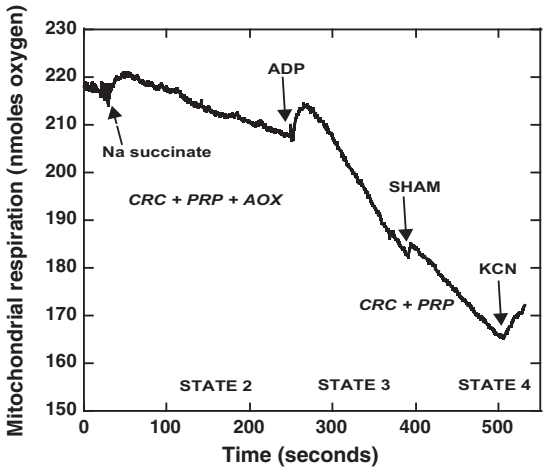

Fig. 7. Respiratory profile of mitochondria isolated from SC5314 *C. albicans* grown in YNB medium. Freshly prepared mitochondria (1 mg/ml) were suspended in respiration buffer (10 mM Tris–HCl pH 6.8, 0.65 M sorbitol, 10 mM KCl, 0.36 mM EDTA) and oxygen consumption was measured with an oxygen electrode at 30 °C. Where indicated, sodium succinate (10 mM) was added as a respiratory substrate and ADP (1 mM) was added to induce oxidative phosphorylation (state 3). SHAM (5 mM) was then added for specific inhibition of the alternative oxidase (AOX) pathway and respiration was stopped by adding 10 mM KCN. CRC is classic respiratory chain, PAR is parallel respiratory chain.

filamentous forms is a consequence and not a cause of the filamentation process (Figs. 1 and 2), as already suggested by previous studies in which GSH/GSSG redox imbalance with reduced hypha forming capability was observed in some oxidative stress resistant *C. albicans* mutants [71,72]. This hypothesis was supported by the results of the dynamics experiments (Fig. 3) in which glutathione content decreased rapidly (within 1 min) in response to new hypha-inducing growth conditions. In addition, the surprisingly high GSSG levels (maybe due to reoxidation after import within the cell) observed in the presence of exogenous GSH could trigger a protein glutathionylation process. On the other hand, the presence of NAC was disturbing thiol metabolism and was not sufficient to allow the cells to filament in hypha-inducing conditions, in agreement with previous work showing that a *C. albicans* γ-GCS mutant could only partly be rescued with NAC [30].

Measurements of glutathione levels in two mutants with an oppositely impaired filamentation process, *ΔΔtup1* and *ΔΔefg1*, provided additional evidence for a correlation between glutathione levels and dimorphism. Cells lacking Efg1, the major regulator of hypha formation [63], grew constitutively in the yeast form in YNB medium, with no significant change in glutathione content compared to the wild-type. In YNB-serum hypha-inducing conditions, no filamentation was observed, associated with glutathione depletion compared to the *ΔΔefg1* grown in YNB (Table 3). These data confirm that glutathione depletion does not involve hyphal production. However, there was a 3-fold increase in glutathione content compared to the wild-type grown in YNB-serum, which could be explained by the fact that cells do not need to use glutathione to form hyphae in the mutant. In spider medium, the data are more complex to interpret since no change in glutathione levels was observed in the mutant.

Cells lacking Tup1 [52], which grow constitutively as long pseudohyphae, had glutathione contents in YNB-serum hypha-inducing conditions that were only one fifth those in control conditions but, again, no significant change was observed when cells were grown in rich semi-synthetic spider medium (Table 3). However, our data on both mutants suggest that genetic perturbation of filamentation pathways can be associated with disturbances in glutathione metabolism.

Zhu et al. recently showed that the quorum-sensing molecule (QSM) farnesol conjugates with intracellular GSH, resulting in total glutathione depletion, oxidative stress and apoptosis in *C. albicans* [64]. In this study, farnesol exposure results in the significant increase in the expression of CDR1 and drop in intracellular glutathione proportional to farnesol concentration and exposure time, which was rescued in the presence of exogenous GSH. Although our experimental conditions vary from this study (in particular time of farnesol exposure and growth medium), in order to keep our experimental conditions homogenous, the addition of farnesol to our cell cultures led to an inhibition of hypha formation and a parallel decrease in intracellular glutathione content (Fig. 4). However, under our conditions, exposure time to farnesol was not sufficient to trigger the apoptosis process observed in [64]. A similar effect was observed in the presence of dodecanol, which also inhibits *C. albicans* filamentation (data not shown). Chemical perturbation of the filamentation pathway using farnesol involves glutathione depletion but does not elicit a signal for filamentation, consistent with other studies [71,72]. However, farnesol can promote ROS generation and

Table 5
Specific activities of ERC complexes.
The specific activities of the ERC complexes were measured in isolated mitochondria, as described in the Materials and methods. The values listed are means ± SD of at least three determinations and Student's *t* test was used to identify significant differences.

Specific activity (units/min/mg protein)			
CRC complexes	YNB	YNB-serum	Spider
I	40.0 ± 11.3	14.5 ± 2.1***	12.0 ± 1.4***
II	27.5 ± 0.7	22.0 ± 4.2	28.5 ± 0.7
IV	442.5 ± 33.2	596.0 ± 101.8	624.5 ± 50.2**

*** $p < 0.001$ *versus* YNB.
** $p < 0.01$ *versus* YNB.

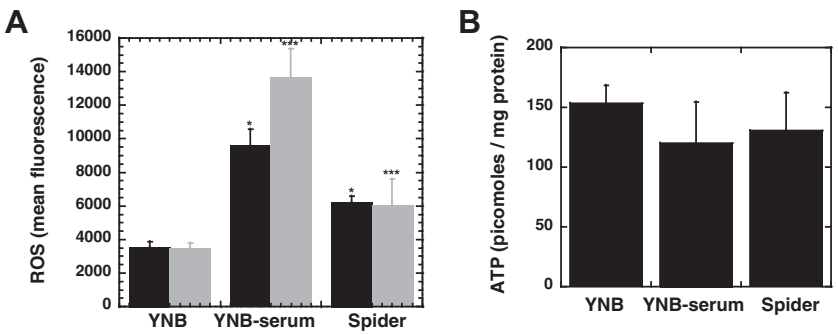

Fig. 8. Flow cytometry assay of ROS and ATP determination. A) Cells were obtained from overnight cultures, washed with PBS, and incubated with the ROS-sensitive fluorescent dye DCFDA (black bars) (at a concentration of 50 μM) for 30 min or with 0.1 mg/ml DHE (gray bars) for 90 min in the dark. They were then subjected to flow cytometry for fluorescence detection. In parallel, background cell fluorescence in the absence of DCFDA and DHE was measured and the value obtained was subtracted from that obtained in each assay. B) ATP was quantified in freshly purified mitochondria with a luminescence kit for ATP determination, with a calibration curve established with various known concentrations of ATP. The results are expressed in pmol ATP/mg protein. All data points in the figure are the means of at least three determinations, normalized with respect to the protein content of the samples, and Student's *t* test was used to identify significant differences ($^{*}p < 0.001$ and $^{**}p < 0.04$ *versus* YNB).

exposure to this chemical should therefore lead to a decrease in glutathione content independent of morphological state [73,74].

By contrast, in the presence of tyrosol, we observed enhanced filamentation and a parallel decrease in glutathione levels in YNB-serum and Spider medium, consistent with the requirement of glutathione for the filamentation process. However, interpretation may be complicated, because QSMs can inhibit multiple processes contributing to filamentation. Overall, our data indicate that the induction of filamentation, either by changing environmental growth conditions (YNB-serum or Spider medium), or by genetic (*ΔΔtup1*) or chemical

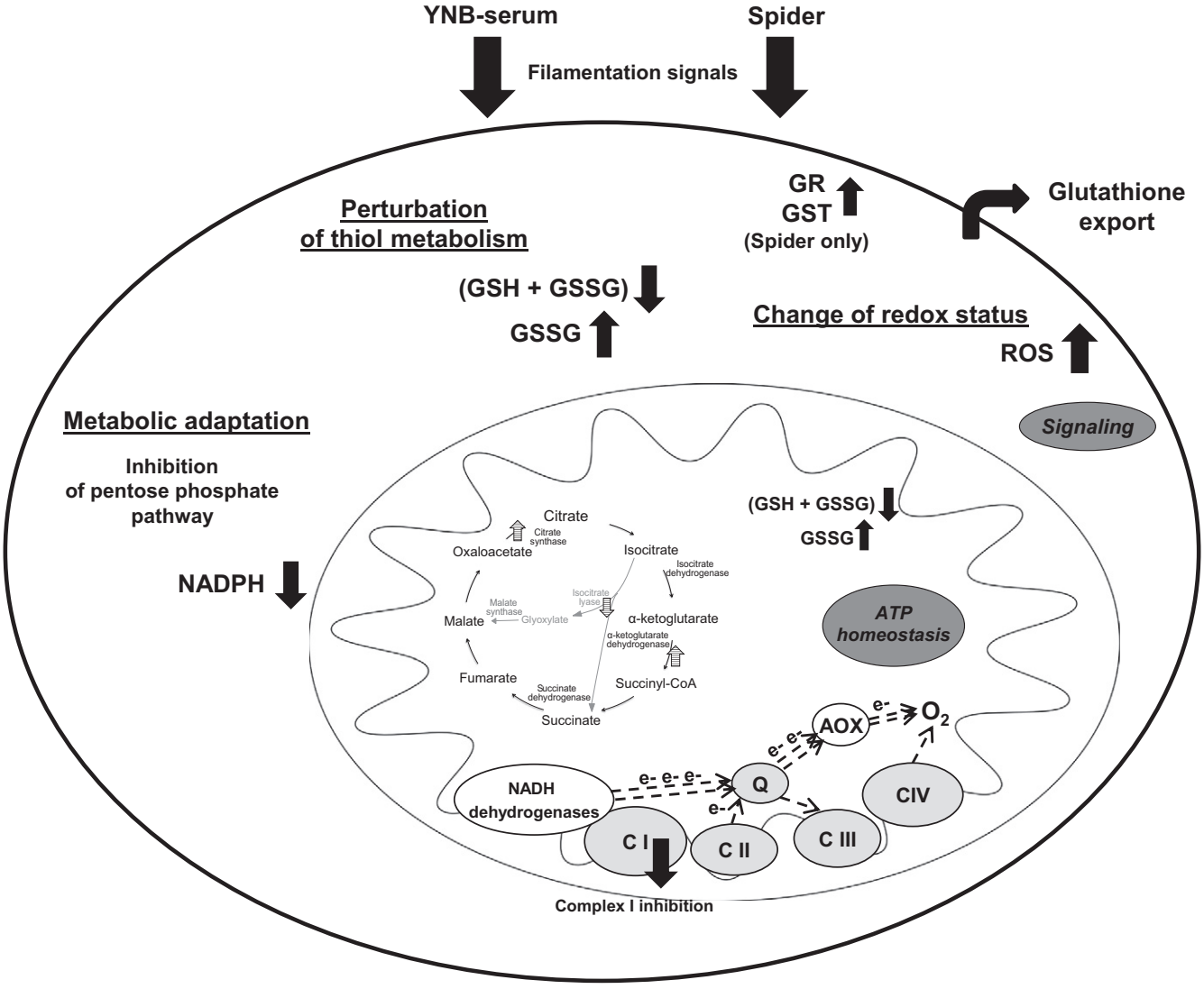

Fig. 9. Schematic representation of the adaptive metabolic pathway during the filamentation process.

(tyrosol) modifications, is systematically associated with a depletion of intracellular glutathione.

Changes in intracellular redox status and intracellular glutathione consumption may be associated with filamentation but what would be the energetic cost of this adaptation? We investigated, in detail, possible changes in mitochondrial function occurring during the yeast-to-hyphae transition. Interest in pathogen carbon metabolism has recently increased, following observations suggesting that at least some host environments are deficient in glucose, and that the cell capacity to assimilate the available nutrients is a major factor in its ability to undergo filamentous growth [75,76]. In addition, it has been shown that hyphal length had a significant impact on the macrophage ability to engulf *C. albicans* cells [12]. Glucose may be catabolized to generate acetyl-CoA for the TCA cycle *via* glycolysis or converted into five-carbon sugars *via* the pentose phosphate pathway. We observed a strong inhibition of the pentose phosphate pathway, NADPH depletion, which was not compensated through IDP cytosolic activity, and an inhibition of the mitochondrial NADP-dependent IDP (Fig. 5). IDP1 has been shown to be induced by interaction with macrophages [13]. These data confirm that changes in redox status parallel metabolic changes tending toward more energetic metabolism.

Consistent with the stimulation of glycolysis, we found that the general activity of the TCA cycle was stimulated (Fig. 6), with greater citrate synthase activity, and a concomitant slight increase in pyruvate dehydrogenase (PDH) complex and a two- to three-fold increase in the activity of KGDH in the two sets of hypha-inducing conditions used in this study. These data are consistent with the previous finding of a filamentation defect in a PDX mutant [49]. Citrate synthase activation drives the TCA cycle toward more energetic metabolism, providing the mitochondrial respiratory chain with a larger number of electrons. This process does not seem to involve the glyoxylate cycle under our culture conditions, because levels of isocitrate lyase activity were very low in YNB-serum and Spider medium (Fig. 6). *C. albicans* has been shown to adapt to environmental conditions through the use of alternative carbon pathways, such as the glyoxylate cycle, in host niches deficient in glucose, such as phagocytes, with a shift from glycolysis to gluconeogenesis, and an upregulation of the principal enzymes of the glyoxylate cycle: isocitrate lyase and malate synthase [13,68,77]. Mutants lacking isocitrate lyase present a filamentation defect and are markedly less virulent in mice than the wild type [13,68]. This response to nutrient starvation is usually followed by a late transcriptional response, corresponding to filamentation and escape from the macrophage, with a return to normal glycolysis activity, as in our experimental conditions. These effects, occurring in parallel with pentose phosphate pathway inhibition, suggest that the signal for hypha formation is derived from the glycolysis system and transmitted to the electron transfer system through the citric acid cycle, as suggested in previous studies [48,49,78]. However, the differences observed in isocitrate lyase activity in our study emphasize the difference between our *in vitro* experiments and *C. albicans* behavior when confronted to macrophages.

Under our hypha-inducing conditions, mitochondrial respiration increased by a factor of three to five in the filamentous forms in the presence of pyruvate/malate as an electron donor. These data confirm the link between *C. albicans* dimorphism and the need for an efficient respiration system for hyphal growth. Moreover, as the use of a pyruvate/malate mixture as an electron donor requires the integrity of the mitochondrial metabolic pathways, these data are consistent with TCA cycle activation. However, in the presence of NADH, which can be oxidized by complex I and/or NADH dehydrogenases, oxygen consumption decreased in both YNB-serum and spider media, and rotenone had a weaker effect (Table 4). These data suggest a different partitioning of electrons between the respiratory chains in filamentous forms.

Studies of mitochondrial respiration in the presence of various ETC inhibitors showed SHAM-dependent respiration levels in the filamentous forms to be twice those in the yeast form, regardless of the substrate used to donate electrons to the respiratory chain. AOX is not sensitive to cyanide, but is inhibited in the presence of SHAM. These data suggest an increase in the contribution of the AOX pathway in hypha-inducing conditions. *C. albicans* can also oxidize cytoplasmic substrates, such as NADH, through external rotenone-insensitive dehydrogenases [41]. In the presence of NADH as an electron donor, rotenone had a weaker inhibitory effect in both filamentous forms, with a parallel decrease in rotenone-sensitive complex I activity (Tables 4 and 5) suggesting an increase in the contribution of the alternative rotenone-insensitive NADH Q-oxidoreductase.

Electron transfer through AOX, NADH dehydrogenases and the parallel respiratory chain produces less ATP than the classical pathway. These alternative pathways have therefore been identified as possible compensatory mechanisms in cases of CRC failure, but previous studies have shown that both CRC and AOX1 are constitutively expressed in fungi [41–43,79,80]. An apparent uncoupling of oxidative phosphorylation in filamentous forms may play a role in the adaptation of cells. However, the inhibition of complex I and an increase in ROS production (Fig. 8) should impair respiration and be detrimental for the cells. We propose that filamentous cells overcome this problem by stimulating the TCA cycle to provide the respiratory chain with more electrons and to increase the proportion of electrons passing through the alternative oxidase and rotenone insensitive-NADH dehydrogenase pathways.

5. Conclusions

We conclude that glutathione is necessary for hyphal formation. The filamentation process results in depletion in intracellular glutathione levels, changes in redox status, apparent oxidative stress, glutathione excretion and protein glutathionylation. Glutathione depletion is thus the price paid by the cells to allow the filamentation to occur. The cells must therefore maintain a fragile intracellular balance (and minimal glutathione limitation) between temporary glutathione-dependent oxidative stress, necessary to hyphal formation, and excessive glutathione depletion. Indeed, additional disturbance might lead to severe oxidative stress, glutathione extrusion and cell apoptosis. Temporary oxidative stress is associated with an increase in ROS production, which may constitute a signal for bioenergetic adaptive strategies. The cellular energetic cost of this response of *C. albicans* cells include bypassing complex I to maintain the rates of respiration and normal ATP levels to cover the metabolic needs of the cells, enabling them to survive the new environmental conditions they may experience within the host.

Supplementary data to this article can be found online at http://dx.doi.org/10.1016/j.bbadis.2014.07.006.

Acknowledgements

This work was supported by grant ANR REDOX PRO from the French National Research Agency.

We would like to thank Dr Sandy Johnson (UCSF, California, USA) for kindly providing us with the *ΔΔTup1* rescue/TUP1-URA3 (Bca02-11 strain).

References

[1] R.A. Calderone, *Candida* and Candidiasis, American Society for Microbiology Press, Washington. DC, 2002.
[2] A.L. Mavor, S. Thewes, B. Hube, Systemic fungal infections caused by *Candida* species: epidemiology, infection process and virulence attributes, Curr. Drug Targets 6 (2005) 863–874.
[3] F.C. Odds, *Candida* and Candidosis, 2nd edition Bailliere Tindall, London, 1988.
[4] J. Berman, Morphogenesis and cell cycle progression in *Candida albicans*, Curr. Opin. Microbiol. 9 (2006) 595–601.
[5] N.A. Gow, Germ tube growth of *Candida albicans*, Curr. Top. Med. Mycol. 8 (1997) 43–55.
[6] P. Sudbery, N. Gow, J. Berman, The distinct morphogenic states of *Candida albicans*, Trends Microbiol. 12 (2004) 317–324.
[7] M. Whiteway, U. Oberholzer, *Candida* morphogenesis and host–pathogen interactions, Curr. Opin. Microbiol. 7 (2004) 350–357.
[8] R.A. Calderone, W.A. Fonzi, Virulence factors of *Candida albicans*, Trends Microbiol. 9 (2001) 327–335.

[9] H.J. Lo, J.R. Kohler, B. DiDomenico, D. Loebenberg, A. Cacciapuoti, G.R. Fink, Nonfilamentous *C. albicans* mutants are avirulent, Cell 90 (1997) 939–949.
[10] A.P. Mitchell, Dimorphism and virulence in *Candida albicans*, Curr. Opin. Microbiol. 1 (1998) 687–692.
[11] D.R. Soll, *Candida* commensalism and virulence: the evolution of phenotypic plasticity, Acta Trop. 81 (2002) 101–110.
[12] L.E. Lewis, J.M. Bain, C. Lowes, C. Gillespie, F.M. Rudkin, N.A. Gow, L.P. Erwig, Stage specific assessment of *Candida albicans* phagocytosis by macrophages identifies cell wall composition and morphogenesis as key determinants, PLoS Pathog. 8 (2012) e1002578.
[13] M.C. Lorenz, J.A. Bender, G.R. Fink, Transcriptional response of *Candida albicans* upon internalization by macrophages, Eukaryot. Cell 3 (2004) 1076–1087.
[14] S. Biswas, P. Van Dijck, A. Datta, Environmental sensing and signal transduction pathways regulating morphopathogenic determinants of *Candida albicans*, Microbiol. Mol. Biol. Rev. 71 (2007) 348–376.
[15] P.E. Sudbery, Growth of *Candida albicans* hyphae, Nat. Rev. Microbiol. 9 (2011) 737–748.
[16] C.L. Taschdjian, J.J. Burchall, P.J. Kozinn, Rapid identification of *Candida albicans* by filamentation on serum and serum substitutes, Am. J. Dis. Child. 99 (1960) 212–215.
[17] J. Buffo, M.A. Herman, D.R. Soll, A characterization of pH-regulated dimorphism in *Candida albicans*, Mycopathologia 85 (1984) 21–30.
[18] D. Mardon, E. Balish, A.W. Phillips, Control of dimorphism in a biochemical variant of *Candida albicans*, J. Bacteriol. 100 (1969) 701–707.
[19] N. Simonetti, V. Strippoli, A. Cassone, Yeast-mycelial conversion induced by N-acetyl-D-glucosamine in *Candida albicans*, Nature 250 (1974) 344–346.
[20] K.L. Lee, H.R. Buckley, C.C. Campbell, An amino acid liquid synthetic medium for the development of mycelial and yeast forms of *Candida albicans*, Sabouraudia 13 (1975) 148–153.
[21] H. Liu, J. Kohler, G.R. Fink, Suppression of hyphal formation in *Candida albicans* by mutation of a STE12 homolog, Science 266 (1994) 1723–1726.
[22] A.J. Brown, N.A. Gow, Regulatory networks controlling *Candida albicans* morphogenesis, Trends Microbiol. 7 (1999) 333–338.
[23] R.S. Shapiro, O. Ryan, C. Boone, L.E. Cowen, Regulatory circuitry governing morphogenesis in *Saccharomyces cerevisiae* and *Candida albicans*, Cell Cycle 11 (2012) 4294–4295.
[24] M. Whiteway, Transcriptional control of cell type and morphogenesis in *Candida albicans*, Curr. Opin. Microbiol. 3 (2000) 582–588.
[25] E. Herrero, J. Ros, G. Belli, E. Cabiscol, Redox control and oxidative stress in yeast cells, Biochim. Biophys. Acta 1780 (2008) 1217–1235.
[26] P. Gonzalez-Parraga, J.A. Hernandez, J.C. Arguelles, Role of antioxidant enzymatic defences against oxidative stress H(2)O(2) and the acquisition of oxidative tolerance in *Candida albicans*, Yeast 20 (2003) 1161–1169.
[27] D.J. Jamieson, D.W. Stephen, E.C. Terriere, Analysis of the adaptive oxidative stress response of *Candida albicans*, FEMS Microbiol. Lett. 138 (1996) 83–88.
[28] A. Meister, M.E. Anderson, Glutathione, Annu. Rev. Biochem. 52 (1983) 711–760.
[29] M.J. Penninckx, An overview on glutathione in *Saccharomyces* versus non-conventional yeasts, FEMS Yeast Res. 2 (2002) 295–305.
[30] Y.U. Baek, Y.R. Kim, H.S. Yim, S.O. Kang, Disruption of gamma-glutamylcysteine synthetase results in absolute glutathione auxotrophy and apoptosis in *Candida albicans*, FEBS Lett. 556 (2004) 47–52.
[31] A.K. Yadav, P.R. Desai, M.N. Rai, R. Kaur, K. Ganesan, A.K. Bachhawat, Glutathione biosynthesis in the yeast pathogens *Candida glabrata* and *Candida albicans*: essential in *C. glabrata*, and essential for virulence in *C. albicans*, Microbiology 157 (2011) 484–495.
[32] P. Gonzalez-Parraga, F.R. Marin, J.C. Arguelles, J.A. Hernandez, Correlation between the intracellular content of glutathione and the formation of germ-tubes induced by human serum in *Candida albicans*, Biochim. Biophys. Acta 1722 (2005) 324–330.
[33] M. Manavathu, S. Gunasekaran, Q. Porte, E. Manavathu, M. Gunasekaran, Changes in glutathione metabolic enzymes during yeast-to-mycelium conversion of *Candida albicans*, Can. J. Microbiol. 42 (1996) 76–79.
[34] D. Thomas, K. Klein, E. Manavathu, J.R. Dimmock, B. Mutus, Glutathione levels during thermal induction of the yeast-to-mycelial transition in *Candida albicans*, FEMS Microbiol. Lett. 61 (1991) 331–334.
[35] P. Gonzalez-Parraga, R. Alonso-Monge, J. Pla, J.C. Arguelles, Adaptive tolerance to oxidative stress and the induction of antioxidant enzymatic activities in *Candida albicans* are independent of the Hog1 and Cap1-mediated pathways, FEMS Yeast Res. 10 (2010) 747–756.
[36] C. Michan, C. Pueyo, Growth phase-dependent variations in transcript profiles for thioredoxin- and glutathione-dependent redox systems followed by budding and hyphal *Candida albicans* cultures, FEMS Yeast Res. 9 (2009) 1078–1090.
[37] A. Garcera, C. Casas, E. Herrero, Expression of *Candida albicans* glutathione transferases is induced inside phagocytes and upon diverse environmental stresses, FEMS Yeast Res. 10 (2010) 422–431.
[38] M.J. Patterson, C.G. McKenzie, D.A. Smith, A. da Silva Dantas, S. Sherston, E.A. Veal, B.A. Morgan, D.M. Maccallum, L.P. Erwig, J. Quinn, Ybp1 and Gpx3 signaling in *Candida albicans* govern hydrogen peroxide-induced oxidation of the Cap1 transcription factor and macrophage escape, Antioxid. Redox Signal. 19 (18) (2013 Dec 20) 2244–2260.
[39] G.M. Chaves, S. Bates, D.M. Maccallum, F.C. Odds, *Candida albicans* GRX2, encoding a putative glutaredoxin, is required for virulence in a murine model, Genet. Mol. Res. 6 (2007) 1051–1063.
[40] R.A. Cavalheiro, F. Fortes, J. Borecky, V.C. Faustinoni, A.Z. Schreiber, A.E. Vercesi, Respiration, oxidative phosphorylation, and uncoupling protein in *Candida albicans*, Braz. J. Med. Biol. Res. 37 (2004) 1455–1461.
[41] E.J. Helmerhorst, M.P. Murphy, R.F. Troxler, F.G. Oppenheim, Characterization of the mitochondrial respiratory pathways in *Candida albicans*, Biochim. Biophys. Acta 1556 (2002) 73–80.
[42] E.J. Helmerhorst, M. Stan, M.P. Murphy, F. Sherman, F.G. Oppenheim, The concomitant expression and availability of conventional and alternative, cyanide-insensitive, respiratory pathways in *Candida albicans*, Mitochondrion 5 (2005) 200–211.
[43] W.K. Huh, S.O. Kang, Molecular cloning and functional expression of alternative oxidase from *Candida albicans*, J. Bacteriol. 181 (1999) 4098–4102.
[44] F.W. Chattaway, R. Bishop, M.R. Holmes, F.C. Odds, A.J. Barlow, Enzyme activities associated with carbohydrate synthesis and breakdown in the yeast and mycelial forms of *Candida albicans*, J. Gen. Microbiol. 75 (1973) 97–109.
[45] G.A. Land, W.C. McDonald, R.L. Stjernholm, T.L. Friedman, Factors affecting filamentation in *Candida albicans*: relationship of the uptake and distribution of proline to morphogenesis, Infect. Immun. 11 (1975) 1014–1023.
[46] W.J. Nickerson, An enzymatic locus participating in cellular division of a yeast, J. Gen. Physiol. 37 (1954) 483–494.
[47] F. Ruy, A.E. Vercesi, A.J. Kowaltowski, Inhibition of specific electron transport pathways leads to oxidative stress and decreased *Candida albicans* proliferation, J. Bioenerg. Biomembr. 38 (2006) 129–135.
[48] J.A. McDonough, V. Bhattacherjee, T. Sadlon, M.K. Hostetter, Involvement of *Candida albicans* NADH dehydrogenase complex I in filamentation, Fungal Genet. Biol. 36 (2002) 117–127.
[49] V.F. Vellucci, S.E. Gygax, M.K. Hostetter, Involvement of *Candida albicans* pyruvate dehydrogenase complex protein X (Pdx1) in filamentation, Fungal Genet. Biol. 44 (2007) 979–990.
[50] A.M. Gillum, E.Y. Tsay, D.R. Kirsch, Isolation of the *Candida albicans* gene for orotidine-5′-phosphate decarboxylase by complementation of *S. cerevisiae* ura3 and *E. coli* pyrF mutations, Mol. Gen. Genet. 198 (1984) 179–182.
[51] D.A. Hudson, Q.L. Sciascia, R.J. Sanders, G.E. Norris, P.J. Edwards, P.A. Sullivan, P.C. Farley, Identification of the dialysable serum inducer of germ-tube formation in *Candida albicans*, Microbiology 150 (2004) 3041–3049.
[52] B.R. Braun, A.D. Johnson, Control of filament formation in *Candida albicans* by the transcriptional repressor TUP1, Science 277 (1997) 105–109.
[53] V.R. Stoldt, A. Sonneborn, C.E. Leuker, J.F. Ernst, Efg1p, an essential regulator of morphogenesis of the human pathogen *Candida albicans*, is a member of a conserved class of bHLH proteins regulating morphogenetic processes in fungi, EMBO J. 16 (1997) 1982–1991.
[54] W.A. Fonzi, M.Y. Irwin, Isogenic strain construction and gene mapping in *Candida albicans*, Genetics 134 (1993) 717–728.
[55] A.L. Bulteau, S. Planamente, L. Jornea, A. Dur, E. Lesuisse, J.M. Camadro, F. Auchère, Changes in mitochondrial glutathione levels and protein thiol oxidation in *Δyfh1* yeast cells and the lymphoblasts of patients with Friedreich's ataxia, Biochim. Biophys. Acta 1822 (2012) 212–225.
[56] F. Galiazzo, A. Schiesser, G. Rotilio, Glutathione peroxidase in yeast. Presence of the enzyme and induction by oxidative conditions, Biochem. Biophys. Res. Commun. 147 (1987) 1200–1205.
[57] W.H. Habig, M.J. Pabst, W.B. Jakoby, Glutathione S-transferases. The first enzymatic step in mercapturic acid formation, J. Biol. Chem. 249 (1974) 7130–7139.
[58] J. Sedlak, R.H. Lindsay, Estimation of total, protein-bound, and nonprotein sulfhydryl groups in tissue with Ellman's reagent, Anal. Biochem. 25 (1968) 192–205.
[59] W. Mailinger, A. Baumeister, M. Reuss, M. Rizzi, Rapid and highly automated determination of adenine and pyridine nucleotides in extracts of *Saccharomyces cerevisiae* using a micro robotic sample preparation-HPLC system, J. Biotechnol. 63 (1998) 155–166.
[60] F. Auchère, R. Santos, S. Planamente, E. Lesuisse, J.M. Camadro, Glutathione-dependent redox status of frataxin-deficient cells in a yeast model of Friedreich's ataxia, Hum. Mol. Genet. 17 (2008) 2790–2802.
[61] L.M. Hinman, J.P. Blass, An NADH-linked spectrophotometric assay for pyruvate dehydrogenase complex in crude tissue homogenates, J. Biol. Chem. 256 (1981) 6583–6586.
[62] J. Reglinski, S. Hoey, W.E. Smith, R.D. Sturrock, Cellular response to oxidative stress at sulfhydryl group receptor sites on the erythrocyte membrane, J. Biol. Chem. 263 (1988) 12360–12366.
[63] B.R. Braun, A.D. Johnson, TUP1, CPH1 and EFG1 make independent contributions to filamentation in *Candida albicans*, Genetics 155 (2000) 57–67.
[64] J. Zhu, B.P. Krom, D. Sanglard, C. Intapa, C.C. Dawson, B.M. Peters, M.E. Shirtliff, M.A. Jabra-Rizk, Farnesol-induced apoptosis in *Candida albicans* is mediated by Cdr1-p extrusion and depletion of intracellular glutathione, PLoS One 6 (2011) e28830.
[65] J.M. Hornby, E.C. Jensen, A.D. Lisec, J.J. Tasto, B. Jahnke, R. Shoemaker, P. Dussault, K. W. Nickerson, Quorum sensing in the dimorphic fungus *Candida albicans* is mediated by farnesol, Appl. Environ. Microbiol. 67 (2001) 2982–2992.
[66] M. Kruppa, Quorum sensing and *Candida albicans*, Mycoses 52 (2009) 1–10.
[67] H. Chen, M. Fujita, Q. Feng, J. Clardy, G.R. Fink, Tyrosol is a quorum-sensing molecule in *Candida albicans*, Proc. Natl. Acad. Sci. U. S. A. 101 (2004) 5048–5052.
[68] M.C. Lorenz, G.R. Fink, Life and death in a macrophage: role of the glyoxylate cycle in virulence, Eukaryot. Cell 1 (2002) 657–662.
[69] M.T. Lin, M.F. Beal, Mitochondrial dysfunction and oxidative stress in neurodegenerative diseases, Nature 443 (2006) 787–795.
[70] J.F. Ernst, D. Tielker, Responses to hypoxia in fungal pathogens, Cell. Microbiol. 11 (2009) 183–190.
[71] A. Fekete, T. Emri, A. Gyetvai, Z. Gazdag, M. Pesti, Z. Varga, J. Balla, C. Cserhati, L. Emody, L. Gergely, I. Pocsi, Development of oxidative stress tolerance resulted in reduced ability to undergo morphologic transitions and decreased pathogenicity in a t-butylhydroperoxide-tolerant mutant of *Candida albicans*, FEMS Yeast Res. 7 (2007) 834–847.
[72] A. Fekete, I. Pocsi, T. Emri, A. Gyetvai, Z. Gazdag, M. Pesti, Z. Karanyi, L. Majoros, L. Gergely, Physiological and morphological characterization of tert-butylhydroperoxide tolerant *Candida albicans* mutants, J. Basic Microbiol. 48 (2008) 480–487.

[73] M.L. Langford, S. Hasim, K.W. Nickerson, A.L. Atkin, Activity and toxicity of farnesol towards *Candida albicans* are dependent on growth conditions, Antimicrob. Agents Chemother. 54 (2010) 940–942.
[74] C. Westwater, E. Balish, D.A. Schofield, *Candida albicans*-conditioned medium protects yeast cells from oxidative stress: a possible link between quorum sensing and oxidative stress resistance, Eukaryot. Cell 4 (2005) 1654–1661.
[75] C.J. Barelle, C.L. Priest, D.M. Maccallum, N.A. Gow, F.C. Odds, A.J. Brown, Niche-specific regulation of central metabolic pathways in a fungal pathogen, Cell. Microbiol. 8 (2006) 961–971.
[76] M.C. Lorenz, Carbon catabolite control in *Candida albicans*: new wrinkles in metabolism, MBio 4 (2013) (e00034–00013).
[77] C. Fradin, P. De Groot, D. MacCallum, M. Schaller, F. Klis, F.C. Odds, B. Hube, Granulocytes govern the transcriptional response, morphology and proliferation of *Candida albicans* in human blood, Mol. Microbiol. 56 (2005) 397–415.
[78] T. Watanabe, A. Ogasawara, T. Mikami, T. Matsumoto, Hyphal formation of *Candida albicans* is controlled by electron transfer system, Biochem. Biophys. Res. Commun. 348 (2006) 206–211.
[79] W.K. Huh, S.O. Kang, Characterization of the gene family encoding alternative oxidase from *Candida albicans*, Biochem. J. 356 (2001) 595–604.
[80] G. Milani, W. Jarmuszkiewicz, C.M. Sluse-Goffart, A.Z. Schreiber, A.E. Vercesi, F.E. Sluse, Respiratory chain network in mitochondria of *Candida* parapsilosis: ADP/O appraisal of the multiple electron pathways, FEBS Lett. 508 (2001) 231–235.